

Model Evaluation in Medical Datasets Over Time

Helen Zhou*

Yuwen Chen*

Zachary C. Lipton

Carnegie Mellon University, Pittsburgh, PA, USA

HLZHOU@ANDREW.CMU.EDU

YUWENC2@ANDREW.CMU.EDU

ZLIPTON@ANDREW.CMU.EDU

Abstract

Machine learning models deployed in healthcare systems face data drawn from continually evolving environments. However, researchers proposing such models typically evaluate them in a time-agnostic manner, with train and test splits sampling patients throughout the entire study period. We introduce the Evaluation on Medical Datasets Over Time (EMDOT) framework and Python package, which evaluates the performance of a model class over time. Across five medical datasets and a variety of models, we compare two training strategies: (1) using all historical data, and (2) using a window of the most recent data. We note changes in performance over time, and identify possible explanations for these shocks.

Keywords: Deployment, distribution shift, evaluation over time

1. Introduction

As medical practices, healthcare systems, and community environments evolve over time, so does the distribution of collected data. Features are deprecated as new ones are introduced, data collection may fluctuate depending on hospital policies, and the underlying populations may shift.

Amidst this ever-changing data landscape, models that perform well on one time period cannot be assumed to perform well in pe-

tuity. In the MIMIC-III critical care dataset, [Nestor et al. \(2019\)](#) found that a change to the electronic health record (EHR) system in 2008 coincided with sudden degradations in AUROC for mortality prediction. Shifts over time may also occur in a more gradual, continuous fashion. In COVID-19 data from the Centers for Disease Control and Prevention (CDC), [Cheng et al. \(2021\)](#) noted that the age distribution among cases shifted continually throughout the pandemic, and that these continual shifts confounded estimates of improvements in mortality rate.

We propose an evaluation framework to characterize model performance over time by simulating training procedures that practitioners could have executed up to each time point, and subsequently deployed in future time points. We argue that standard time-agnostic evaluation is insufficient for selecting deployment-ready models, showing that it over-estimates deployment performance. Instead, we advocate for EMDOT as a worthwhile pre-deployment step to help practitioners gain confidence in the robustness of their models to distribution shifts that have happened in the past and may to some extent repeat in the future.

While intuitive, evaluation of models over time remains far from standard practice in the development of machine learning models for healthcare (ML4H). One possible reason for this is lack of access—as noted by [Nestor et al. \(2019\)](#), it is common practice to re-

* equal contribution

move timestamps when de-identifying medical datasets for public use. In this work, we identify five sources of medical data containing varying granularities of temporal information per-record, four of which are *publicly available*. We profile the performance of various training strategies and model classes across time, and identify possible sources of distribution shifts within each dataset. We release the Evaluation on Medical Datasets Over Time (EMDOT) Python package¹ (details in Appendix A) to allow researchers to apply EMDOT to their own datasets and test techniques for handling shifts over time.

2. Related work

The promise of ML for improving healthcare has been explored in several domains, from cancer survival prediction (Hegselmann et al., 2018), to diabetic retinopathy detection (Gulshan et al., 2016), to antimicrobial stewardship (Kanjilal et al., 2020; Boominathan et al., 2020), to mortality prediction in liver transplant candidates (Byrd et al., 2021). Typically, these ML models are evaluated on a random held-out set of patients, and sometimes externally validated on other hospitals or newly collected data. However, what makes a model trustworthy enough to be deployed in the wild?

The medical community has a long history of utilizing (mostly) fixed, simple risk scores to inform patient care (Six et al., 2008; Kamath et al., 2001; Wilson et al., 1998; Wells et al., 1995). Risk scores often prioritize ease-of-use, are computed from few variables, verified by domain experts for clear causal connections to outcomes of interest, and validated through use over time and across hospitals. Together, these factors give clinicians confidence that the model will perform reliably for years to come. With increasingly complex models, however, trust and adop-

tion may be hindered by a lack of confidence in robustness to changing environments.

As noted by D’Amour et al. (2020), ML models often exhibit unexpectedly poor behavior when deployed in real-world domains. A key reason for this, they argue, is *under-specification*, where ML pipelines yield many predictors with equivalently strong held-out performance in the training domain, but such predictors can behave very differently in deployment. EMDOT could stress test models to help combat under-specification.

Although evaluation over time is far from standard in ML4H literature, some have begun to explore this idea. To predict wound-healing, Jung and Shah (2015) found that when data were split by cutoff time instead of patients, benefits of model averaging and stacking disappeared. Pianykh et al. (2020) found degradation in performance of a model for wait times dependent on how much historical data was trained on. To predict severe COVID-19, Zhou et al. (2022) found that learned clinical concept features performed more robustly over time than raw features.

Closest to our work is Nestor et al. (2019), which evaluated AUROC in MIMIC-III from 2003–2012, comparing training on just 2001–2002; the prior year; and the full history. Using the full history and manual aggregations of clinical concepts, they bridged a big drop in performance due to changing EHR systems. Whereas Nestor et al. (2019) considers three models per test year, EMDOT simulates model deployment every year and evaluates across *all future years*.

EMDOT shares similarities to techniques for cross-validation in time series forecasting (Bergmeir and Benítez, 2012; Cerqueira et al., 2020), but instead of just reporting summary statistics that could conceal shifts over time, EMDOT seeks to elucidate the nature and potential causes of fluctuating performance over time. Also, we evaluate models treating data as i.i.d. (not longitudinal).

1. github.com/acmi-lab/EvaluationOverTime

Table 1: Summary of datasets used for analysis. For more details, see Appendices B–F.

Dataset name	Outcome	Time Range (time point unit)	# samples	# positives
SEER (Breast)	5-year Survival	1975–2013 (year)	462,023	378,758
SEER (Colon)	5-year Survival	1975–2013 (year)	254,112	135,065
SEER (Lung)	5-year Survival	1975–2013 (year)	457,695	49,997
CDC COVID-19	Mortality	Mar 2020–May 2022 (month)	941,140	190,786
SWPA COVID-19	90-day Mortality	Mar 2020–Feb 2022 (month)	35,293	1,516
MIMIC-IV	In-ICU Mortality	2009–2020 (year)	53,050	3,334
OPTN (Liver)	180-day Mortality	2005–2017 (year)	143,709	4,635

3. Data

We sought medical datasets that had (1) a timestamp for each record, (2) interesting prediction task(s), and (3) enough distinct time points to evaluate over. Five datasets satisfied these criteria: SEER cancer data, national CDC COVID-19 data, COVID-19 data from a major provider in Southwestern Pennsylvania (SWPA), MIMIC-IV critical care data, and OPTN liver transplant data. All but SWPA are publicly accessible.

Table 1 summarizes the data. Figure 1 visualizes data quantity over time. Appendices B–F include cohort selection diagrams, cohort characteristics, features, heat maps of missingness, preprocessing steps, and additional details. Finally, each sample corresponds to a distinct patient.

4. Methods

We compare the *reported* test performance of a model if it were trained using standard (all-period) time-agnostic splits to more realistic performance from simulating how a practitioner might have trained and deployed models in the past (evaluation over time). We consider both linear and more complex model classes, as well as two training regimes: (1) when models are trained on a recent window of the past, and (2) models are trained on all historical data. Finally, we describe diagnostic plots, which help detect reasons for changing model performance.

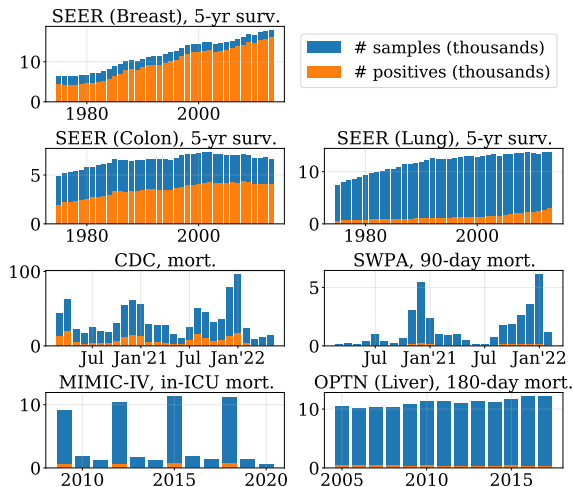


Figure 1: Number of samples and positive outcomes per time point.

Prediction Task All tasks are binary classification, evaluated by AUROC. Samples are treated in an ‘i.i.d.’ manner for training.

All-Period Training We mimic common practice by using time-agnostic data splits, which randomly place samples from the entire study time range into train, validation, and test sets (Appendix K).

Evaluation over Time Training To simulate how practitioners train models and subsequently deploy them on future data, we define the EMDOT framework. At each time point (“simulated deployment date”), an *in-period* set of data is available for model development. Evaluation is on both recent in-period and future *out-of-period* data.

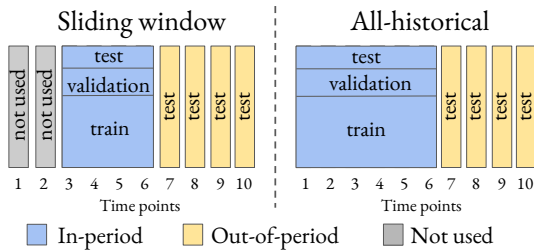


Figure 2: EMDOT training regimes.

In-period data is split into train, validation, and test sets (ratios and hyperparameters in Appendices K and J). Recent in-period performance is evaluated on held-out test data from the most recent time point. Out-of-period performance is evaluated on all data from each future time point. E.g., a model trained up to time 6 is tested on data from 6, 7, 8, etc. (Figure 2), and at time 8, the model is two time points *stale*. This procedure can take $\leq T$ times more computation than all-period training for T time points.

Practitioners face a tradeoff between using recent data reflective of the present and using all available historical data for a larger sample size. Intuitively, the former may be appealing in modern applications with massive datasets, whereas the latter may be necessary in data-scarce applications. We explore these two training regimes, with different definitions of in-period data (Figure 2):

1. **Sliding window:** The last W time points are in-period. Here, $W = 4$ for sufficient positive examples.
2. **All-historical:** Any data prior to the current time point is in-period.

To decouple the effect of sample size from that of distribution shifts, we also perform comparisons with all-historical data that is **sub-sampled** to be the same size as the corresponding sliding window training set.

Models Logistic regression (LR), gradient boosted decision trees (GBDT) and feedforward neural networks (MLP) are compared.

Detecting Sources of Change To better understand possible reasons for changing performance, we create *diagnostic plots* to track importances and average values of the most important features over time. We generate these plots for logistic regression and define feature importance by the magnitudes of the coefficients, but note that other feature importance techniques could be used for more complex model classes. By highlighting sudden changes in the performance and the corresponding time periods, diagnostic plots surface shifts in the distribution of data that coincide with changing model performance.

5. Results

Here, we focus on three datasets with interesting results: SEER (Colon), CDC, and SWPA. Full results are in the Appendix.

All-period Training In standard time-agnostic evaluation, on all datasets except MIMIC-IV, GBDT and MLP perform best (Table 2, Appendix Table 19). Top 10 coefficients of LR models are in Appendices B–F.

Table 2: Test AUROC in all-period training.

Model	SEER (Colon)	CDC	SWPA
LR	0.867	0.837	0.914
GBDT	0.871	0.850	0.926
MLP	0.873	0.844	0.918

Evaluation Over Time Figures 3 and 43 (Appendix) plot AUROC of LR over time using all-historical data. (GBDT, MLP, AUPRC, F1, and accuracy in Appendix I.)

The test performance of a model from standard all-period training (red dotted line) mostly sits above the performance of any model that could have been realistically been deployed by that date. Thus, all-period training tends to provide an over-optimistic estimate of performance at deployment.

In SEER data, AUROC increases dramatically near 1988, but several of the subsequent models see a large drop around 2003 (Figure 3). By contrast, in CDC data, model performance is relatively smooth over time. Models trained after December 2020 have a slight boost in AUROC, coinciding with a surge in cases (and hence sample size, Figure 1). In SWPA COVID-19, there is more variation and uncertainty in AUROC early in the pandemic, where sample sizes are small. In December 2020, sample sizes increase, and models seem to become more robust to changes over time. In all data, in-sample test AUROCs tend to increase over time.

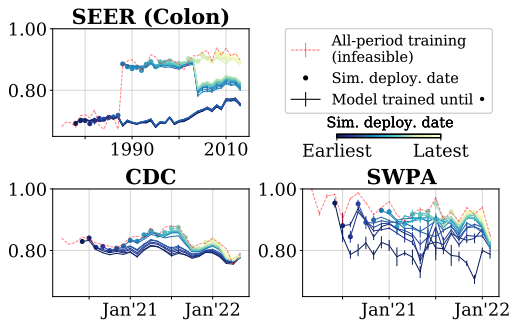


Figure 3: LR average test AUROC vs. time. Solid line = model from a sim. deploy. date (dot), evaluated on future times. Error bars are std. dev. over 5 random splits. Dotted line is infeasible, as it trains on data after sim. deploy. date.

Training Regime Comparison Training regimes perform differently depending on the dataset (Figure 4 and Appendix Figure 44, left). In CDC COVID-19, sliding window outperforms all-historical across all stalenesses. By contrast, in SWPA COVID-19, which has the least amount of data (Table 1), both sliding window and all-historical (subsampled) underperform all-historical. In SEER (Colon), performance is relatively stable regardless of training regime.

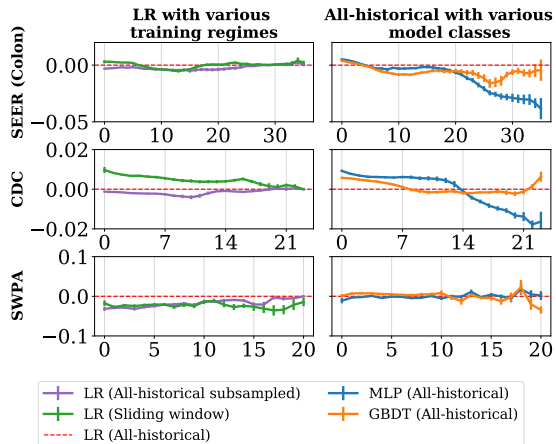


Figure 4: AUROC - AUROC_{LR All-historical} vs. staleness, with various training regimes (left) and model classes (right). Error bars are \pm std. dev.

Model Comparison In SEER (Colon) and CDC COVID-19, both GBDT and MLP initially outperform LR when staleness is < 4 years and < 7 months (respectively), but both eventually underperform LR as staleness increases further (Figure 4, right). In SWPA COVID-19, all model classes perform comparably over time. In MIMIC-IV, LR remained the best (Appendix Figure 44, right).

Detecting Possible Sources of Change Diagnostic plots for all datasets are in Appendix H. Here, we discuss SEER (Lung) (Figure 5) in detail. In 1983, as EOD 4 features (extent of disease coding schema) are introduced, a sudden jump in AUROC occurs. However, models trained at this time later experience a large AUROC drop. By 1988, EOD 4 is phased out, and EOD 10 features are introduced. This coincides with another jump in AUROC, sustained until 2003 when the EOD 10 features are removed. In this dataset, the all-historical training regime seems more robust to changes over time, as all-historical models trained after 1988 avoid the drop that sliding window models undergo once their window excludes pre-1988 data.

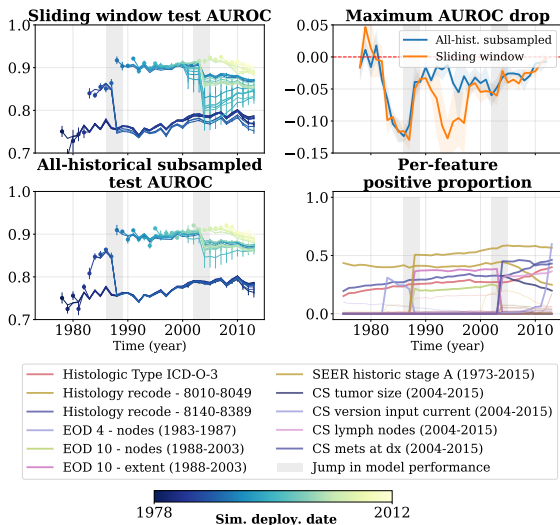


Figure 5: SEER (Lung) diagnostic plots. AUROC vs. time (left), max. drop in AUROC for each simulated deployment time (top right), and prevalences of the most important features over time (bottom right).

6. Discussion

As standard all-period training evaluates performance on time points already seen in the training set, the reported performance tends to be over-optimistic (Figure 3) and does not reflect degradation that would have occurred in deployment. Comparing model classes, in all datasets except MIMIC-IV, GBDT and MLP outperform LR under standard time-agnostic evaluation (Appendix Table 19). However, evaluated across time, LR is often comparable and even outperforms more complex models once enough time passes after the simulated deployment date (e.g. LR eventually overtaking MLP in SEER Breast, Colon, and Lung; Figure 4).

Sample size can influence which training regime performs better. In SWPA COVID-19 (smallest dataset), the sliding window and sub-sampled all-historical training regimes perform comparably, both underperforming

all-historical (Figure 4). Here, the benefit of larger sample size in all-historical outweighs the potential issue of stale data clouding the fresh data distribution. On the other hand, in CDC COVID-19 (largest dataset), subsampled all-historical performs comparably to all-historical, and sliding window outperforms both across all stalenesses (Figure 4). Here, the performance of LR may have been saturated even when a sub-sample of all-historical data was used, and the benefit of using more recent data outweighs the larger sample size afforded by all-historical. In rapidly evolving environments, the sliding window training regime may be advantageous, as long as there is enough data.

The SEER datasets had dramatic changes in data distribution in both 1988 and 2003, when important features were added and/or removed (Figure 5). One possible reason for the robustness of all-historical models in this dataset is that after 2003, when features like EOD 10 were removed, the model could still rely on features that were introduced prior to the use of EOD 10 in 1988. More broadly, we hypothesize that if a model was trained on a mixture of distributions that occurred throughout the past, it may be better equipped to handle shifts to settings similar to those distributions in the future.

In conclusion, EMDOT not only explores the suitability of different model classes or training regimes for deployment, but also helps one detect distribution shifts that occurred in the past. Understanding such shifts may help practitioners be prepared for shifts of a similar nature in the future.

Future Work To alleviate concerns about computation time, we plan to add parallelization to EMDOT. Another interesting extension is exploring other data modalities (e.g. images). More broadly, we hope that others may build upon EMDOT to shine new light on how models fare when evaluated with an eye towards deployment.

References

- Christoph Bergmeir and José M. Benítez. On the use of cross-validation for time series predictor evaluation. *Information Sciences*, 191:192–213, 2012. ISSN 0020-0255. doi: <https://doi.org/10.1016/j.ins.2011.12.028>. URL <https://www.sciencedirect.com/science/article/pii/S0020025511006773>. Data Mining for Software Trustworthiness.
- Sooraj Nath Boominathan, Michael Oberst, Helen Zhou, Sanjat Kanjilal, and David Sontag. Treatment policy learning in multiobjective settings with fully observed outcomes. In *Proceedings of the 26th ACM SIGKDD International Conference on Knowledge Discovery & Data Mining, KDD '20*, page 1937–1947, New York, NY, USA, 2020. Association for Computing Machinery. ISBN 9781450379984. doi: [10.1145/3394486.3403245](https://doi.org/10.1145/3394486.3403245). URL <https://doi.org/10.1145/3394486.3403245>.
- Jonathon Byrd, Sivaraman Balakrishnan, Xiaoqian Jiang, and Zachary C Lipton. Predicting mortality in liver transplant candidates. In *Explainable AI in Healthcare and Medicine*, pages 321–333. Springer, 2021.
- Centers for Disease Control and Prevention. COVID-19 Case Surveillance Restricted Access Detailed Data, May 2020.
- Vitor Cerqueira, Luis Torgo, and Igor Mozetič. Evaluating time series forecasting models: An empirical study on performance estimation methods. *Machine Learning*, 109(11):1997–2028, 2020.
- Cheng Cheng, Helen Zhou, Jeremy C Weiss, and Zachary C Lipton. Unpacking the drop in covid-19 case fatality rates: A study of national and florida line-level data. In *AMIA Annual Symposium Proceedings*, volume 2021, page 285. American Medical Informatics Association, 2021.
- Mehee Choi, Clifton D Fuller, Charles R Thomas Jr, and Samuel J Wang. Conditional survival in ovarian cancer: results from the seer dataset 1988–2001. *Gynecologic oncology*, 109(2):203–209, 2008.
- Alexander D’Amour, Katherine Heller, Dan Moldovan, Ben Adlam, Babak Alipanahi, Alex Beutel, Christina Chen, Jonathan Deaton, Jacob Eisenstein, Matthew D Hoffman, et al. Underspecification presents challenges for credibility in modern machine learning. *arXiv preprint arXiv:2011.03395*, 2020.
- Clifton D Fuller, Samuel J Wang, Charles R Thomas Jr, Henry T Hoffman, Randal S Weber, and David I Rosenthal. Conditional survival in head and neck squamous cell carcinoma: results from the seer dataset 1973–1998. *Cancer: Interdisciplinary International Journal of the American Cancer Society*, 109(7):1331–1343, 2007.
- Varun Gulshan, Lily Peng, Marc Coram, Martin C Stumpe, Derek Wu, Arunachalam Narayanaswamy, Subhashini Venugopalan, Kasumi Widner, Tom Madams, Jorge Cuadros, Ramasamy Kim, Rajiv Raman, Philip Q Nelson, Jessica Mega, and Dale Webster. Development and validation of a deep learning algorithm for detection of diabetic retinopathy in retinal fundus photographs. *JAMA*, 2016. URL <http://jamanetwork.com/journals/jama/fullarticle/2588763>.
- Stefan Hegselmann, Leonard Gruelich, Julian Varghese, and Martin Dugas. Reproducible survival prediction with seer cancer data. In *Machine Learning for Health-*

- care Conference*, pages 49–66. PMLR, 2018.
- Alistair Johnson, Lucas Bulgarelli, Tom Pollard, Steven Horng, Leo Anthony Celi, and Roger Mark. Mimic-iv, 2021. URL <https://physionet.org/content/mimiciv/1.0/>.
- Kenneth Jung and Nigam H Shah. Implications of non-stationarity on predictive modeling using ehrs. *Journal of biomedical informatics*, 58:168–174, 2015.
- Patrick S Kamath, Russell H Wiesner, Michael Malinchoc, Walter Kremers, Terry M Therneau, Catherine L Kosberg, Gennaro D’Amico, E Rolland Dickson, and W Ray Kim. A model to predict survival in patients with end-stage liver disease. *Hepatology*, 33(2):464–470, 2001.
- Sanjat Kanjilal, Michael Oberst, Sooraj Boominathan, Helen Zhou, David C Hooper, and David Sontag. A decision algorithm to promote outpatient antimicrobial stewardship for uncomplicated urinary tract infection. *Science Translational Medicine*, 12(568):eaay5067, 2020.
- Surveillance Research Program National Cancer Institute, DCCPS. Seer research data, 9 registries, nov 2020 sub (1975-2018) - linked to county attributes - time dependent (1990-2019) income/rurality, 1969-2020 counties, Nov 2020.
- Bret Nestor, Matthew BA McDermott, Willie Boag, Gabriela Berner, Tristan Naumann, Michael C Hughes, Anna Goldenberg, and Marzyeh Ghassemi. Feature robustness in non-stationary health records: caveats to deployable model performance in common clinical machine learning tasks. In *Machine Learning for Healthcare Conference*, pages 381–405. PMLR, 2019.
- Oleg S Pianykh, Georg Langs, Marc Dewey, Dieter R Enzmann, Christian J Herold, Stefan O Schoenberg, and James A Brink. Continuous learning ai in radiology: implementation principles and early applications. *Radiology*, 297(1):6–14, 2020.
- Surveillance Research Program. National cancer institute seer* stat software. *Surveillance Research Program*, 2015.
- AJ Six, BE Backus, and JC Kelder. Chest pain in the emergency room: value of the heart score. *Netherlands Heart Journal*, 16(6):191–196, 2008.
- Emanuela Taioli, Andrea S Wolf, Marlene Camacho-Rivera, Andrew Kaufman, Dong-Seok Lee, Daniel Nicastrì, Kenneth Rosenzweig, and Raja M Flores. Determinants of survival in malignant pleural mesothelioma: a surveillance, epidemiology, and end results (SEER) study of 14,228 patients. *PloS one*, 10(12):e0145039, 2015.
- PhilipS Wells, Jack Hirsh, DavidR Anderson, AnthonyW A Lensing, Gary Foster, Clive Kearon, Jeffrey Weitz, Robert D’Ovidio, Alberto Cogo, Paolo Prandoni, et al. Accuracy of clinical assessment of deep-vein thrombosis. *The Lancet*, 345(8961):1326–1330, 1995.
- Peter WF Wilson, Ralph B D’Agostino, Daniel Levy, Albert M Belanger, Halit Silbershatz, and William B Kannel. Prediction of coronary heart disease using risk factor categories. *Circulation*, 97(18):1837–1847, 1998.
- Helen Zhou, Cheng Cheng, Kelly J. Shields, Gursimran Kochhar, Tariq Cheema, Zachary C. Lipton, and Jeremy C. Weiss. Learning clinical concepts for predicting risk of progression to severe covid-19, 2022. URL <https://arxiv.org/abs/2208.13126>.

Appendix A. EMDOT Python Package

Figure 6 illustrates the workflow of the EMDOT Python package.

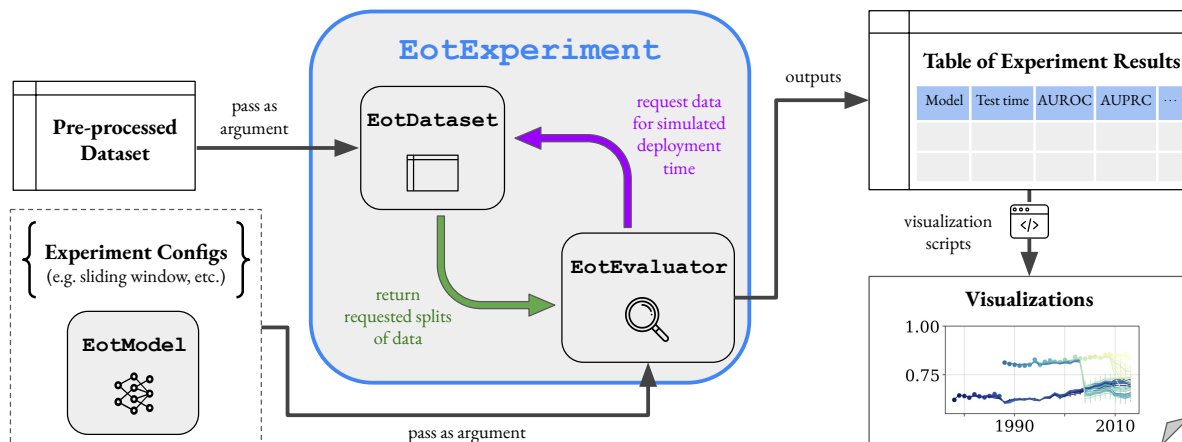


Figure 6: EMDOT Python package workflow diagram. The primary touchpoint of the EMDOT package is the `EotExperiment` object. Users provide a dataframe for their (mostly) preprocessed dataset (EMDOT takes care of normalization based on the relevant training set), their desired experiment configuration (e.g. sliding window), and model class (which should subclass the simple `EotModel` abstract class) in order to create an `EotExperiment` object. Running the `run_experiment()` function of the `EotExperiment` returns a dataframe of experiment results that can then be visualized. The diagram also provides insight into some of the internals of the `EotExperiment` object – there is an `EotDataset` object that handles data splits, and an `EotEvaluator` object that executes the main evaluation loop.

Appendix B. Additional SEER Data Details

The Surveillance, Epidemiology, and End Results (SEER) Program collects cancer incidence data from registries throughout the U.S. This data has been used to study survival in several forms of cancer (Choi et al., 2008; Fuller et al., 2007; Taioli et al., 2015; Hegselmann et al., 2018). Each case includes demographics, primary tumor site, tumor morphology, stage and diagnosis, first course of treatment, and survival outcomes (collected with follow-up) (National Cancer Institute, 2020). The performance over time is evaluated on a *yearly* basis. We use the November 2020 version of the SEER database with nine registries (SEER 9), which covers about 9.4% of the U.S. population. While there are SEER databases that aggregate over more registries and hence cover a greater proportion of the U.S. population, we choose SEER 9 due to the large time range it covers (1975–2018).

- Data access: After filling out a Data Use Agreement and Best Practices Agreement, individuals can easily request access to the SEER dataset.
- Cohort selection: Using the SEER*Stat software (Program, 2015), we define three cohorts of interest: (1) breast cancer, (2) colon cancer, and (3) lung cancer. We primarily follow the cohort selection procedure from Hegselmann et al. (2018), but we use SEER 9 instead of SEER 18, and use data from all available years instead of limiting to 2004–2009. Cohort selection diagrams are given in Figures 7, 8, and 9. If there are multiple samples per patient, we filter to the first entry per patient, which corresponds to when a patient first enters the dataset. This corresponds to a particular interpretation of the prediction: when a patient is first added to a cancer registry, given what we know about that patient, what is their estimated 5-year survival probability?
- Cohort characteristics: Summaries of the SEER (Breast), SEER (Colon), and SEER (Lung) cohort characteristics are in Tables 3, 4, and 5.
- Outcome definition: 5-year survival is defined by a confirmation that the patient is alive five years after the year of diagnosis.
- Features: We list the features used in the SEER breast, colon, and lung cancer datasets in Section B.2. For all datasets, we convert all categorical variables into dummy features, and apply standard scaling to numerical variables (subtract mean and divide by standard deviation).
- Missingness heat maps: are given in Figures 10, 11, 12, 13, 14, and 15.

B.1. Cohort Selection and Cohort Characteristics

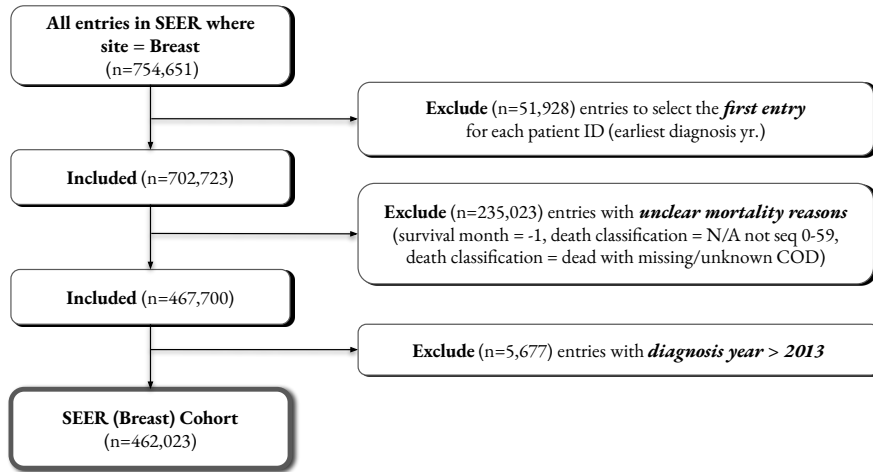


Figure 7: Cohort selection diagram - SEER (Breast)

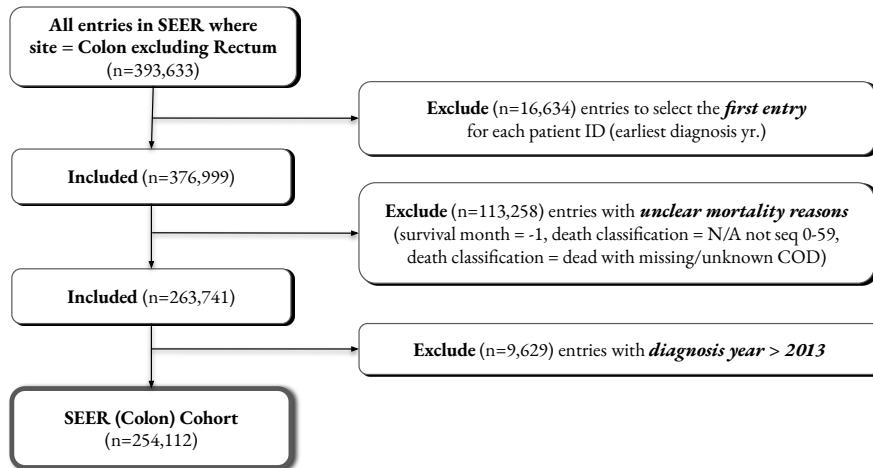


Figure 8: Cohort selection diagram - SEER (Colon)

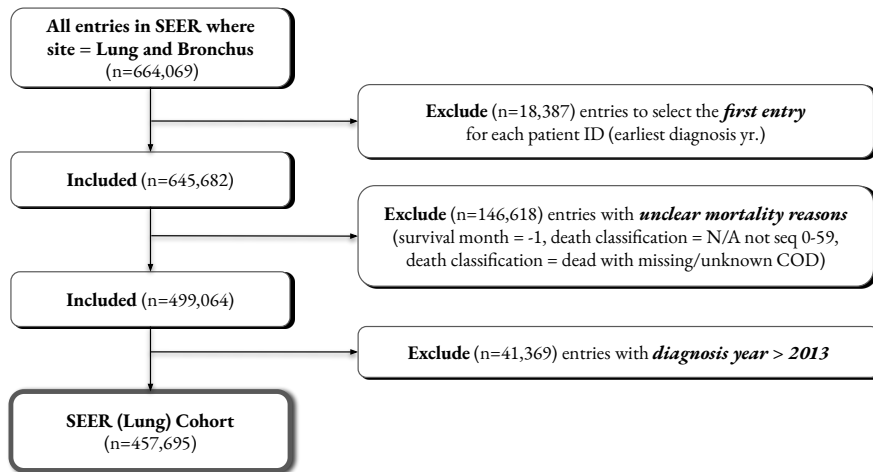


Figure 9: Cohort selection diagram - SEER (Lung)

Table 3: SEER (Breast) cohort characteristics, with count (%) or median (Q1 – Q3).

Characteristic		Missingness	Type
Sex			
Female	459,184 (99.4%)	–	categorical
Male	2,839 (0.6%)	–	categorical
Age recode with single ages and 85+	60 (50-71)	0.0%	continuous
Race/ethnicity			
White	387,247 (83.8%)	–	categorical
Black	40,217 (8.7%)	–	categorical
Other	34,559 (7.5%)	–	categorical
Laterality			
Right - origin of primary	224,777 (48.7%)	–	categorical
Left - origin of primary	233,549 (50.5%)	–	categorical
Other	3,697 (0.8%)	–	categorical
Regional nodes positive (1988+)	0 (0-3)	21.0%	continuous
T value - based on AJCC 3rd (1988-2003)	10 (10-20)	56.2%	categorical
Derived AJCC T, 7th ed (2010-2015)	13 (13-20)	85.3%	categorical
CS site-specific factor 3 (2004-2017 varying by schema)	0 (0-2)	64.8%	categorical
Regional nodes examined (1988+)	8 (2-15)	21.0%	continuous
Coding system-EOD (1973-2003)			
Four-digit EOD (1983-1987)	44,066 (9.5%)	–	categorical
Ten-digit EOD (1988-2003)	202,450 (43.8%)	–	categorical
Thirteen-digit (expanded) site specific EOD (1973-1982)	52,742 (11.4%)	–	categorical
Blank(s)	162,765 (35.2%)	–	categorical
CS version input original (2004-2015)	10,401 (10,300-20,302)	64.8%	categorical
CS version input current (2004-2015)	20,520 (20,510-20,540)	64.8%	categorical
EOD 10 - extent (1988-2003)	10 (10-13)	56.2%	categorical
Grade (thru 2017)			
Unknown	130,713 (28.3%)	–	categorical
Moderately differentiated; Grade II	135,970 (29.4%)	–	categorical
Poorly differentiated; Grade III	119,900 (26.0%)	–	categorical
Undifferentiated; anaplastic; Grade IV	8,081 (1.7%)	–	categorical
Well differentiated; Grade I	67,359 (14.6%)	–	categorical
SEER historic stage A (1973-2015)			
Regional	136,207 (29.5%)	–	categorical
Localized	286,927 (62.1%)	–	categorical
Unstaged	9,242 (2.0%)	–	categorical
Distant	29,647 (6.4%)	–	categorical
IHS Link			
Record sent for linkage, no IHS match	409,058 (88.5%)	–	categorical
Record sent for linkage, IHS match	1,505 (0.3%)	–	categorical
Blank(s)	51,460 (11.1%)	–	categorical
Histologic Type ICD-O-3	8,500 (8,500-8,500)	0.0%	categorical
EOD 10 - size (1988-2003)	18 (10-30)	56.2%	categorical
Type of Reporting Source			
Hospital inpatient/outpatient or clinic	450,801 (97.6%)	–	categorical
Other	11,222 (2.4%)	–	categorical
SEER cause-specific death classification			
Alive or dead of other cause	378,758 (82.0%)	–	categorical
Dead (attributable to this cancer dx)	83,265 (18.0%)	–	categorical
Survival months	135 (74-220)	0.0%	categorical
5-year survival			
1	378,758 (82.0%)	–	categorical
0	83,265 (18.0%)	–	categorical

Table 4: SEER (Colon) cohort characteristics, with count (%) or median (Q1–Q3).

Characteristic		Missingness	Type
Sex			
Female	133,661 (52.6%)	–	categorical
Male	120,451 (47.4%)	–	categorical
Age recode with single ages and 85+	70 (61-79)	0.0%	continuous
Race recode (White, Black, Other)			
White	212,265 (83.5%)	–	categorical
Black	24,041 (9.5%)	–	categorical
Other	17,806 (7.0%)	–	categorical
CS version input current (2004-2015)	20,510 (20,510-20,540)	72.8%	categorical
Derived AJCC T, 6th ed (2004-2015)	30 (20-40)	73.3%	categorical
Histology ICD-O-2	8,140 (8,140-8,210)	0.0%	categorical
IHS Link			
Record sent for linkage, no IHS match	208,802 (82.2%)	–	categorical
Record sent for linkage, IHS match	744 (0.3%)	–	categorical
Blank(s)	44,566 (17.5%)	–	categorical
Histology recode - broad groupings			
8140-8389: adenomas and adenocarcinomas	213,193 (83.9%)	–	categorical
8440-8499: cystic, mucinous and serous neoplasms	28,257 (11.1%)	–	categorical
8010-8049: epithelial neoplasms, NOS	8,797 (3.5%)	–	categorical
Other	3,865 (1.5%)	–	categorical
Regional nodes positive (1988+)	1 (0-10)	29.8%	continuous
CS mets at dx (2004-2015)	0 (0-22)	72.8%	continuous
Reason no cancer-directed surgery			
Surgery performed	223,929 (88.1%)	–	categorical
Not recommended	13,003 (5.1%)	–	categorical
Other	17,180 (6.8%)	–	categorical
Derived AJCC T, 6th ed (2004-2015)	30 (20-40)	73.3%	categorical
CS version input original (2004-2015)	10,401 (10,300-20,302)	72.8%	categorical
Primary Site	184 (182-187)	0.0%	categorical
Diagnostic Confirmation			
Positive histology	244,616 (96.3%)	–	categorical
Radiography without microscopic confirm	4,822 (1.9%)	–	categorical
Other	4,674 (1.8%)	–	categorical
EOD 10 - extent (1988-2003)	45 (40-85)	57.0%	categorical
Histologic Type ICD-O-3	8,140 (8,140-8,210)	0.0%	categorical
EOD 10 - size (1988-2003)	55 (35-999)	57.0%	categorical
CS lymph nodes (2004-2015)	0 (0-210)	72.8%	categorical
SEER cause-specific death classification			
Dead (attributable to this cancer dx)	119,047 (46.8%)	–	categorical
Alive or dead of other cause	135,065 (53.2%)	–	categorical
Survival months	68 (12-151)	0.0%	categorical
5-year survival			
1	135,065 (53.2%)	–	categorical
0	119,047 (46.8%)	–	categorical

Table 5: SEER (Lung) cohort characteristics, with count (%) or median (Q1 – Q3).

Characteristic		Missingness	Type
Sex			
Female	187,967 (41.1%)	–	categorical
Male	269,728 (58.9%)	–	categorical
Age recode with single ages and 85+	68 (60-76)	0.0%	continuous
Race recode (White, Black, Other)			
White	384,184 (83.9%)	–	categorical
Black	47,237 (10.3%)	–	categorical
Other	26,274 (5.7%)	–	categorical
Histologic Type ICD-O-3	8,070 (8,041-8,140)	0.0%	categorical
Laterality			
Left - origin of primary	178,661 (39.0%)	–	categorical
Right - origin of primary	245,321 (53.6%)	–	categorical
Paired site, but no information concerning laterality	23,196 (5.1%)	–	categorical
Other	10,517 (2.3%)	–	categorical
EOD 10 - nodes (1988-2003)	2 (1-9)	56.3%	categorical
EOD 4 - nodes (1983-1987)	3 (0-9)	88.4%	categorical
Type of Reporting Source			
Hospital inpatient/outpatient or clinic	445,606 (97.4%)	–	categorical
Other	12,089 (2.6%)	–	categorical
SEER historic stage A (1973-2015)			
Regional	79,409 (17.3%)	–	categorical
Distant	182,467 (39.9%)	–	categorical
Blank(s)	123,161 (26.9%)	–	categorical
Localized	50,375 (11.0%)	–	categorical
Unstaged	22,283 (4.9%)	–	categorical
CS version input current (2004-2015)	20,520 (20,510-20,540)	70.6%	categorical
CS mets at dx (2004-2015)	23 (0-40)	70.6%	continuous
CS version input original (2004-2015)	10,401 (10,300-20,302)	70.6%	categorical
CS tumor size (2004-2015)	50 (29-999)	70.6%	categorical
EOD 10 - size (1988-2003)	80 (35-999)	56.3%	categorical
CS lymph nodes (2004-2015)	200 (0-200)	70.6%	categorical
Histology recode - broad groupings			
8140-8389: adenomas and adenocarcinomas	147,127 (32.1%)	–	categorical
8010-8049: epithelial neoplasms, NOS	179,848 (39.3%)	–	categorical
8440-8499: cystic, mucinous and serous neoplasms	6,266 (1.4%)	–	categorical
Other	124,454 (27.2%)	–	categorical
EOD 10 - extent (1988-2003)	78 (40-85)	56.3%	categorical
SEER cause-specific death classification			
Alive or dead of other cause	49,997 (10.9%)	–	categorical
Dead (attributable to this cancer dx)	407,698 (89.1%)	–	categorical
Survival months	7 (2-19)	0.0%	categorical
5-year survival			
1	49,997 (10.9%)	–	categorical
0	407,698 (89.1%)	–	categorical

B.2. Features

SEER (Breast):

AJCC stage 3rd edition (1988-2003)
 AYA site recode/WHO 2008
 Age recode with single ages and 85+
 Behavior code ICD-0-2
 Behavior code ICD-0-3
 Behavior recode for analysis
 Breast - Adjusted AJCC 6th M (1988-2015)
 Breast - Adjusted AJCC 6th N (1988-2015)
 Breast - Adjusted AJCC 6th Stage (1988-2015)
 Breast - Adjusted AJCC 6th T (1988-2015)
 Breast Subtype (2010+)
 CS Schema - AJCC 6th Edition
 CS extension (2004-2015)
 CS lymph nodes (2004-2015)
 CS mets at dx (2004-2015)
 CS site-specific factor 1 (2004-2017 varying by schema)
 CS site-specific factor 15 (2004-2017 varying by schema)
 CS site-specific factor 2 (2004-2017 varying by schema)
 CS site-specific factor 25 (2004-2017 varying by schema)
 CS site-specific factor 3 (2004-2017 varying by schema)
 CS site-specific factor 4 (2004-2017 varying by schema)
 CS site-specific factor 5 (2004-2017 varying by schema)
 CS site-specific factor 6 (2004-2017 varying by schema)
 CS site-specific factor 7 (2004-2017 varying by schema)
 CS tumor size (2004-2015)
 CS version derived (2004-2015)
 CS version input current (2004-2015)
 CS version input original (2004-2015)
 Coding system-EDD (1973-2003)
 Derived AJCC M, 6th ed (2004-2015)
 Derived AJCC M, 7th ed (2010-2015)
 Derived AJCC N, 6th ed (2004-2015)
 Derived AJCC N, 7th ed (2010-2015)
 Derived AJCC Stage Group, 6th ed (2004-2015)
 Derived AJCC Stage Group, 7th ed (2010-2015)
 Derived AJCC T, 6th ed (2004-2015)
 Derived AJCC T, 7th ed (2010-2015)
 Derived HER2 Recode (2010+)
 EOD 10 - extent (1988-2003)
 EOD 10 - nodes (1988-2003)
 EOD 10 - size (1988-2003)
 ER Status Recode Breast Cancer (1990+)
 First malignant primary indicator
 Grade (thru 2017)
 Histologic Type ICD-0-3
 Histology recode - Brain groupings
 Histology recode - broad groupings
 ICCS site rec extended ICD-0-3/WHO 2008
 IHS Link
 Laterality
 Lymphoma subtype recode/WHO 2008 (thru 2017)
 M value - based on AJCC 3rd (1988-2003)
 N value - based on AJCC 3rd (1988-2003)
 Origin recode NHIA (Hispanic, Non-Hisp)
 PR Status Recode Breast Cancer (1990+)
 Primary Site
 Primary by international rules
 Race recode (W, B, AI, API)
 Race recode (White, Black, Other)
 Race/ethnicity
 Regional nodes examined (1988+)
 Regional nodes positive (1988+)
 SEER historic stage A (1973-2015)
 SEER modified AJCC stage 3rd (1988-2003)
 Sex
 Site recode ICD-0-3/WHO 2008
 T value - based on AJCC 3rd (1988-2003)
 Tumor marker 1 (1990-2003)
 Tumor marker 2 (1990-2003)
 Tumor marker 3 (1998-2003)
 Type of Reporting Source

SEER (Colon):

Age recode with <1 year olds
 Age recode with single ages and 85+
 Behavior code ICD-0-2
 Behavior code ICD-0-3
 CS extension (2004-2015)
 CS lymph nodes (2004-2015)
 CS mets at dx (2004-2015)
 CS site-specific factor 1 (2004-2017 varying by schema)

CS tumor size (2004-2015)
 CS version input current (2004-2015)
 CS version input original (2004-2015)
 Derived AJCC M, 6th ed (2004-2015)
 Derived AJCC M, 7th ed (2010-2015)
 Derived AJCC N, 6th ed (2004-2015)
 Derived AJCC N, 7th ed (2010-2015)
 Derived AJCC Stage Group, 6th ed (2004-2015)
 Derived AJCC Stage Group, 7th ed (2010-2015)
 Derived AJCC T, 6th ed (2004-2015)
 Derived AJCC T, 7th ed (2010-2015)
 Diagnostic Confirmation
 EOD 10 - extent (1988-2003)
 EOD 10 - nodes (1988-2003)
 EOD 10 - size (1988-2003)
 Histologic Type ICD-0-3
 Histology ICD-0-2
 Histology recode - broad groupings
 IHS Link
 Origin recode NHIA (Hispanic, Non-Hisp)
 Primary Site
 Primary by international rules
 RX Summ--Surg Prim Site (1998+)
 Race recode (White, Black, Other)
 Reason no cancer-directed surgery
 Regional nodes positive (1988+)
 SEER modified AJCC stage 3rd (1988-2003)
 Sex

SEER (Lung):

AYA site recode/WHO 2008
 Age recode with <1 year olds
 Age recode with single ages and 85+
 Behavior code ICD-0-2
 Behavior code ICD-0-3
 CS extension (2004-2015)
 CS lymph nodes (2004-2015)
 CS mets at dx (2004-2015)
 CS site-specific factor 1 (2004-2017 varying by schema)
 CS tumor size (2004-2015)
 CS version input current (2004-2015)
 CS version input original (2004-2015)
 Derived AJCC M, 6th ed (2004-2015)
 Derived AJCC M, 7th ed (2010-2015)
 Derived AJCC N, 6th ed (2004-2015)
 Derived AJCC N, 7th ed (2010-2015)
 Derived AJCC Stage Group, 6th ed (2004-2015)
 Derived AJCC T, 6th ed (2004-2015)
 Derived AJCC T, 7th ed (2010-2015)
 EOD 10 - extent (1988-2003)
 EOD 10 - nodes (1988-2003)
 EOD 10 - size (1988-2003)
 EOD 4 - nodes (1983-1987)
 First malignant primary indicator
 Grade (thru 2017)
 Histologic Type ICD-0-3
 Histology recode - broad groupings
 ICCS site recode 3rd edition/IARC 2017
 ICCS site recode extended 3rd edition/IARC 2017
 IHS Link
 Laterality
 Origin recode NHIA (Hispanic, Non-Hisp)
 Primary by international rules
 Race recode (White, Black, Other)
 SEER historic stage A (1973-2015)
 Sex
 Type of Reporting Source

B.3. Missingness heatmaps

This section plots missingness heatmaps of categorical and numerical features in each SEER dataset over time. Darker color means larger proportion of missing data.

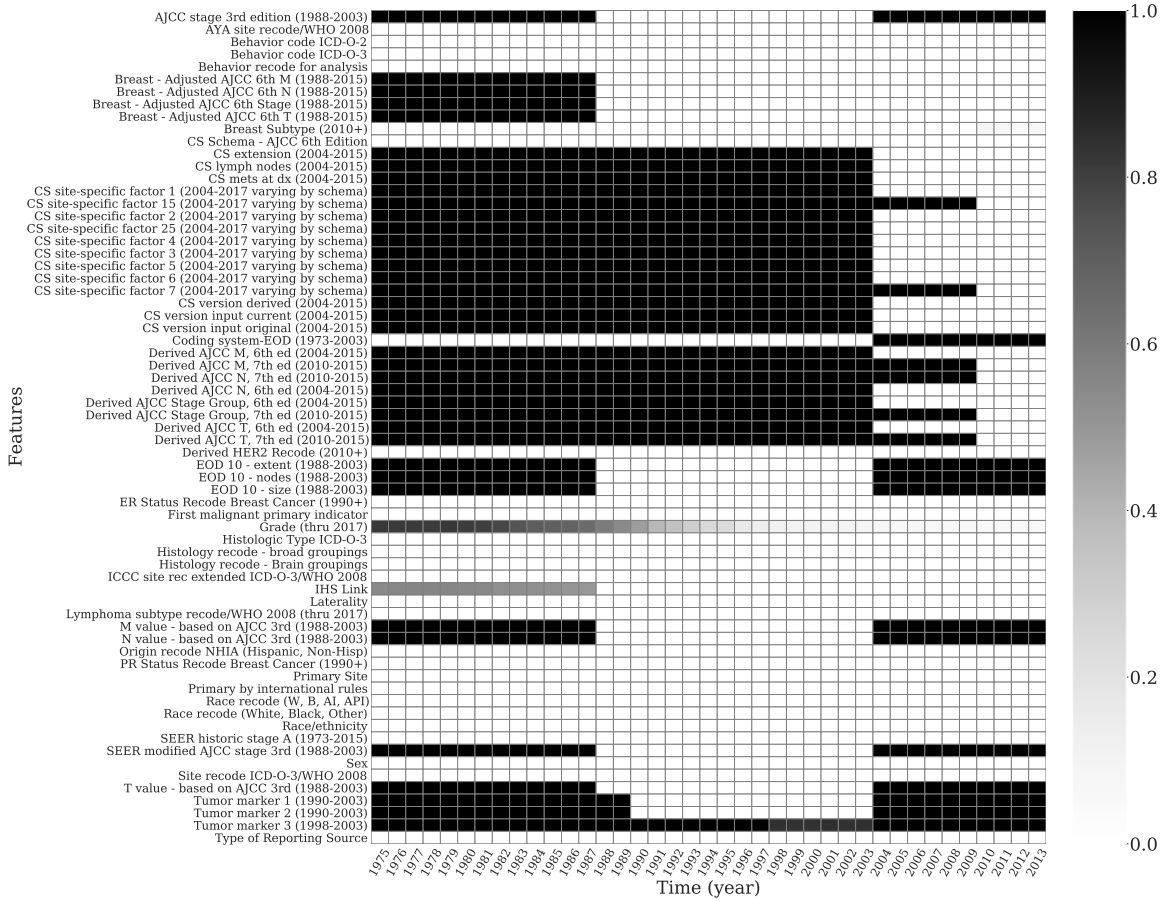


Figure 10: Missingness of categorical features in SEER (Breast).

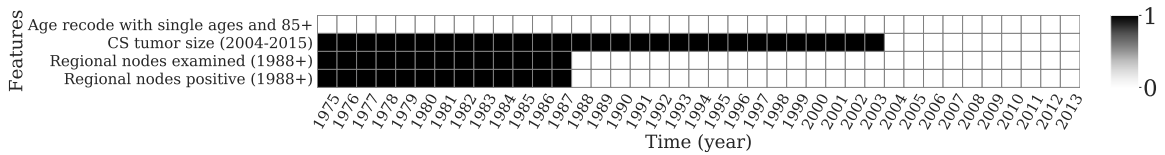


Figure 11: Missingness of numerical features in SEER (Breast).

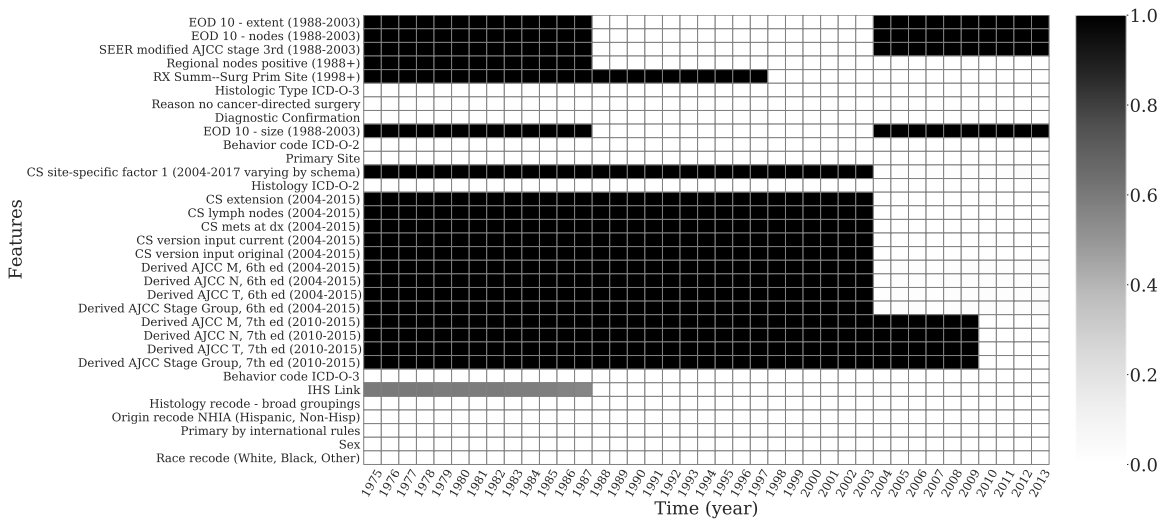


Figure 12: Missingness of categorical features in SEER (Colon).

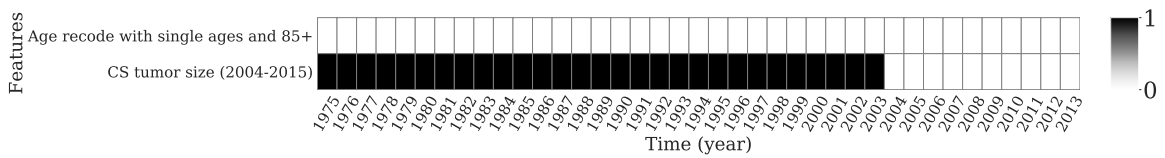


Figure 13: Missingness of numerical features in SEER (Colon).

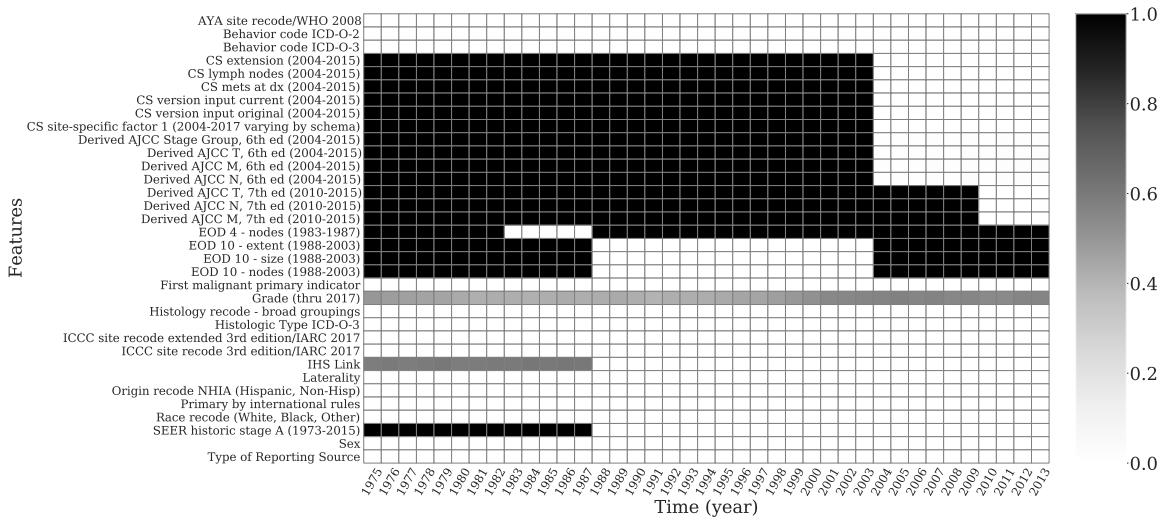


Figure 14: Missingness of categorical features in SEER (Lung).

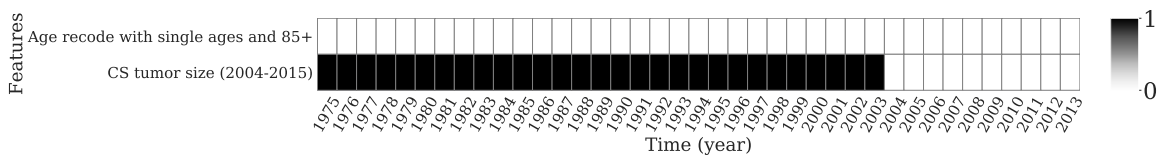


Figure 15: Missingness of numerical features in SEER (Lung).

Appendix C. Additional CDC COVID-19 Data Details

The COVID-19 Case Surveillance Detailed Data ([Centers for Disease Control and Prevention, 2020](#)) is a national, publicly available dataset provided by the CDC. It contains 33 elements, with patient-level data including symptoms, demographics, and state of residence. The performance over time is evaluated on a *monthly* basis. We use the version the released on June 6th, 2022.

- First, a disclaimer: “The CDC does not take responsibility for the scientific validity or accuracy of methodology, results, statistical analyses, or conclusions presented.”
- Data access: To access the data, users must complete a registration information and data use restrictions agreement (RIDURA).
- Cohort selection: The cohort consists of all patients who were lab-confirmed positive for COVID-19, had a non-null positive specimen date, and were hospitalized (`hosp_yn = Yes`). Cohort selection diagrams are given in [Figures 16](#)
- Cohort characteristics: Cohort characteristics are given in [Table 6](#).
- Outcome definition: mortality, defined by `death_yn = Yes`
- Features: We list the features used in the CDC COVID-19 datasets in [Section C.2](#). We convert all categorical variables into dummy features, and apply standard scaling to numerical variables (subtract mean and divide by standard deviation).
- Missingness heat map: is given in [Figure 17](#).
- Additionally, we provide stacked area plots showing how the distribution of ages ([Figure 18\(a\)](#)) and states [18\(b\)](#) shifts over time.

C.1. Cohort Selection and Cohort Characteristics

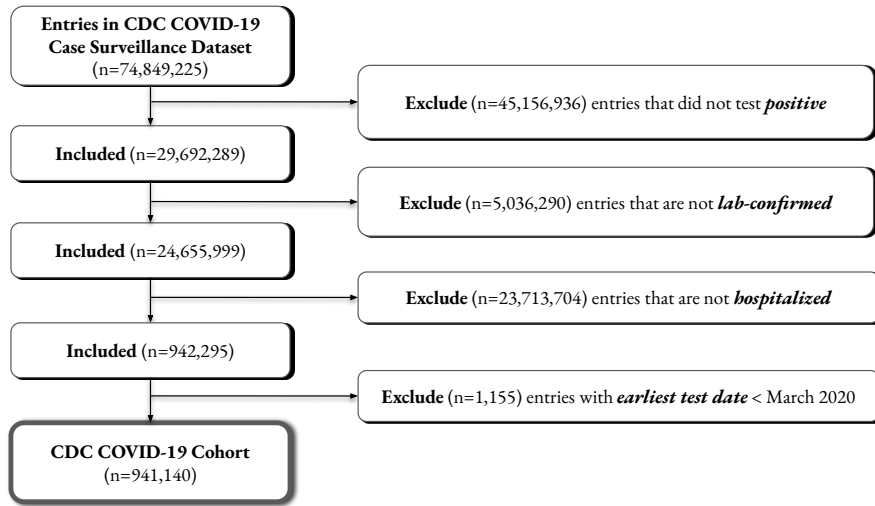


Figure 16: Cohort selection diagram - CDC COVID-19

Table 6: CDC COVID-19 cohort characteristics, with count (%) or median (Q1–Q3).

Characteristic		Missingness	Type
Sex			
Female	455,376 (48.4%)	–	categorical
Male	475,223 (50.5%)	–	categorical
Unknown/Missing	10,541 (1.1%)	–	categorical
Age Group			
0 - 9	16,373 (1.7%)	–	categorical
10 - 19	17,252 (1.8%)	–	categorical
20 - 29	48,505 (5.2%)	–	categorical
30 - 39	71,776 (7.6%)	–	categorical
40 - 49	88,531 (9.4%)	–	categorical
50 - 59	141,805 (15.1%)	–	categorical
60 - 69	189,354 (20.1%)	–	categorical
70 - 79	189,018 (20.1%)	–	categorical
80+	177,765 (18.9%)	–	categorical
Missing	761 (0.1%)	–	categorical
Race			
White	544,199 (57.8%)	–	categorical
Black	173,847 (18.5%)	–	categorical
Other	205,547 (21.8%)	–	categorical
State of Residence			
NY	189,684 (20.2%)	–	categorical
OH	70,097 (7.4%)	–	categorical
FL	35,679 (3.8%)	–	categorical
WA	58,854 (6.3%)	–	categorical
MA	31,441 (3.3%)	–	categorical
Other	555,353 (59.0%)	–	categorical
Mechanical Ventilation			
Yes	38,009 (4.0%)	–	categorical
No	138,331 (14.7%)	–	categorical
Unknown/Missing	764,800 (81.2%)	–	categorical
Mortality			
1	190,786 (20.3%)	–	categorical
0	750,354 (79.7%)	–	categorical

C.2. Features

abdom_yn, abxchest_yn, acuterespdistress_yn, age_group, chills_yn, cough_yn, diarrhea_yn, ethnicity, fever_yn, hc_work_yn, headache_yn, hosp_yn, icu_yn, mechvent_yn, medcond_yn, month, myalgia_yn, nauseavomit_yn, pna_yn, race, relative_month, res_county, res_state, runnose_yn, sex, sfever_yn, sob_yn, sthroat_yn,

C.3. Missingness heatmaps

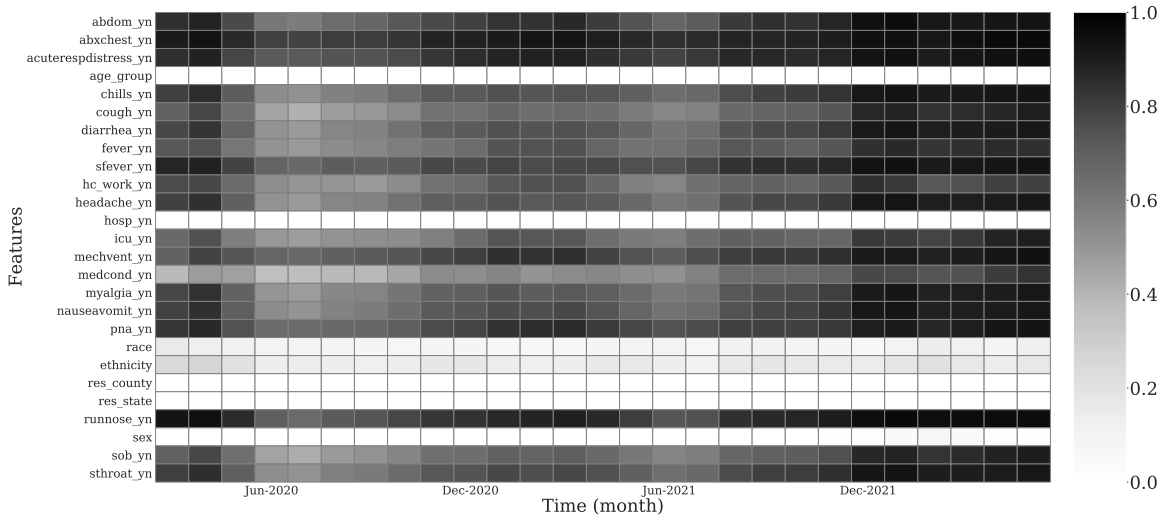


Figure 17: Missingness over time for features in CDC COVID-19 dataset after cohort selection. The darker the color, the larger the proportion of missing data.

C.4. Additional Figures

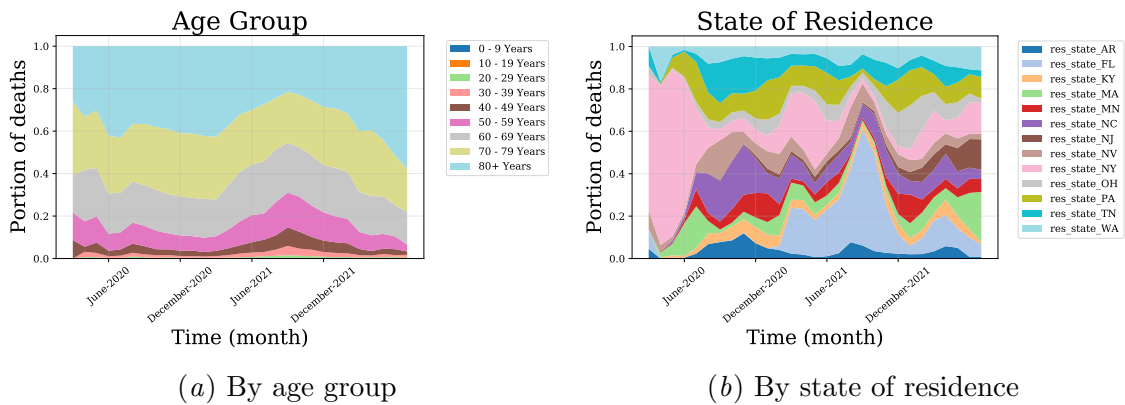


Figure 18: Proportion of deaths over time for each age group and state of residence.

Appendix D. Additional SWPA COVID-19 Data Details

The Southwestern Pennsylvania (SWPA) COVID-19 dataset consists of EHR data from patients tested for COVID-19. It was collected by a major healthcare provider in SWPA (Zhou et al., 2022), and includes patient demographics, labs, problem histories, medications, inpatient vs. outpatient status, and other information collected in the patient encounter. The performance over time is evaluated on a *monthly* basis.

- Data access: This is a private dataset.
- Cohort selection: The cohort consists of COVID-19 patients who tested positive for COVID-19 and were not already in the ICU or mechanically ventilated. We filter for the first positive test, and define features and outcomes relative to that time. Cohort selection diagrams are given in Figures 19. If there are multiple samples per patient, we filter to the first entry per patient, which corresponds to when a patient first enters the dataset. This corresponds to a particular interpretation of the prediction: when a patient is first tests positive, given what we know about that patient, what is their estimated risk of 90-day mortality?
- Cohort characteristics: Cohort characteristics are given in Table 7.
- Outcome definition: 90-day mortality by comparing the death date and test date
- Features: We list the features used in the SWPA COVID-19 datasets in Section D.2. We convert all categorical variables into dummy features, and apply standard scaling to numerical variables (subtract mean and divide by standard deviation). To create a fixed length feature vector, where applicable we take the most recent value of each feature (e.g. most recent lab values).
- Missingness heat maps: are given in Figures 20, 21, 22, and 23,

D.1. Cohort Selection and Cohort Characteristics

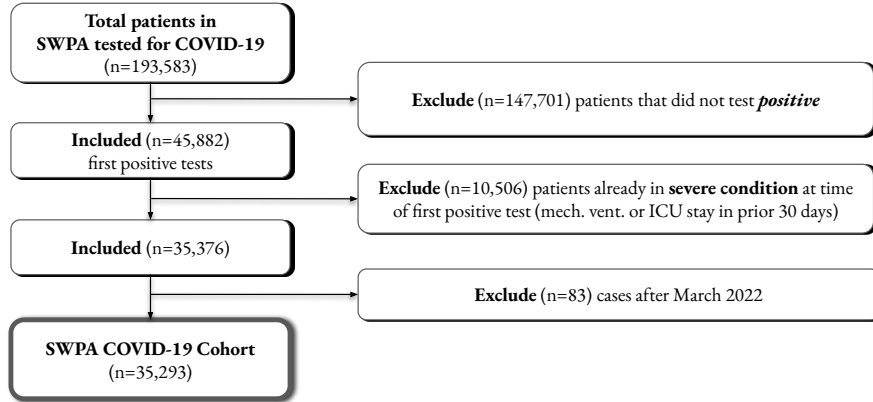


Figure 19: Cohort selection diagram - SWPA COVID-19

Table 7: SWPA COVID-19 cohort characteristics, with count (%) or median (Q1–Q3).

Characteristic		Missingness	Type
Gender			
Female	20,283 (57.5%)	–	categorical
Male	15,003 (42.5%)	–	categorical
Unknown	7 (0.0%)	–	categorical
Age			
Under 20	3,210 (9.1%)	–	categorical
20 – 30	4,349 (12.3%)	–	categorical
30 – 40	4,667 (13.2%)	–	categorical
40 – 50	4,653 (13.2%)	–	categorical
50 – 60	6,111 (17.3%)	–	categorical
60 – 70	5,700 (16.2%)	–	categorical
70+	6,603 (18.7%)	–	categorical
Location of test			
Inpatient	14,911 (42.2%)	–	categorical
Outpatient	17,661 (50.0%)	–	categorical
Unknown	2,721 (7.7%)	–	categorical
90-day mortality			
True	1,516 (4.3%)	–	categorical
False	33,777 (95.7%)	–	categorical

D.2. Features

Asthma	lab_MEAN PLATELET VOLUME
CAD	lab_MONOCYTES ABSOLUTE COUNT
CHF	lab_MONOCYTES RELATIVE PERCENT
CKD	lab_NEUTROPHILS RELATIVE PERCENT
COPD	lab_NUCLEATED RED BLOOD CELLS
CRP	lab_POTASSIUM
CVtest_ICD_Acute pharyngitis, unspecified	lab_PROTEIN TOTAL
CVtest_ICD_Acute upper respiratory infection, unspecified	lab_Q-T INTERVAL
CVtest_ICD_Anosmia	lab_QRS DURATION
CVtest_ICD_Contact with and (suspected) exposure to other viral communicable diseases	lab_QTC CALCULATION
CVtest_ICD_Encounter for general adult medical examination without abnormal findings	lab_RED CELL DISTRIBUTION WIDTH
CVtest_ICD_Encounter for screening for other viral diseases	lab_SODIUM
CVtest_ICD_Encounter for screening for respiratory disorder NEC	lab_VENTRICULAR RATE
CVtest_ICD_Nasal congestion	lab_merged_CRP
CVtest_ICD_Other general symptoms and signs	lab_merged_albumin
CVtest_ICD_Other specified symptoms and signs involving the circulatory and respiratory systems	lab_merged_alkalinePhosphatase
CVtest_ICD_Pain, unspecified	lab_merged_alt
CVtest_ICD_Parageusia	lab_merged_ast
CVtest_ICD_R05.9	lab_merged_bnp
CVtest_ICD_R51.9	lab_merged_ddimer
CVtest_ICD_U07.1	lab_merged_directBilirubin
CVtest_ICD_Viral infection, unspecified	lab_merged_ggt
CVtest_ICD_Z20.822	lab_merged_hct
ESLD	lab_merged_hgb
Hypertension	lab_merged_indirectBilirubin
IP_ICD_z20.828	lab_merged_lactate
Immunocompromised	lab_merged_ldh
Interstitial Lung disease	lab_merged_mcv
OP_ICD_Abdominal Pain	lab_merged_neutrophil
OP_ICD_Chest Pain	lab_merged_platelets
OP_ICD_Chills	lab_merged_pt
OP_ICD_Coronavirus Concerns	lab_merged_rbc
OP_ICD_Covid Infection	lab_merged_sao2
OP_ICD_Exposure To Covid-19	lab_merged_totalBilirubin
OP_ICD_Generalized Body Aches	lab_merged_totalProtein
OP_ICD_Headache	lab_merged_troponin
OP_ICD_Labs Only	lab_merged_wbc
OP_ICD_Medication Refill	labs_ICD_Acute pharyngitis, unspecified
OP_ICD_Nasal Congestion	labs_ICD_Acute upper respiratory infection, unspecified
OP_ICD_Nausea	labs_ICD_Chest pain, unspecified
OP_ICD_Other	labs_ICD_Contact with and (suspected) exposure to other viral communicable diseases
OP_ICD_Results	labs_ICD_Dyspnea, unspecified
OP_ICD_Shortness of Breath	labs_ICD_Encounter for other preprocedural examination
OP_ICD_Sore Throat	labs_ICD_Essential (primary) hypertension
OP_ICD_URI	labs_ICD_Fever, unspecified
age_bin_(20, 30]	labs_ICD_Heart failure, unspecified
age_bin_(30, 40]	labs_ICD_Other general symptoms and signs
age_bin_(40, 50]	labs_ICD_Other pulmonary embolism without acute cor pulmonale
age_bin_(50, 60]	labs_ICD_Other specified abnormalities of plasma proteins
age_bin_(60, 70]	labs_ICD_R05.9
age_bin_(70, 200]	labs_ICD_Shortness of breath
bmi	labs_ICD_Syncope and collapse
cancer	labs_ICD_U07.1
cough	labs_ICD_Unspecified atrial fibrillation
covid_vaccination_given	labs_ICD_Viral infection, unspecified
diabetes	labs_ICD_Z20.822
fatigue	liver disease
fever	location_covidtest_ordered_Inpatient
gender	location_covidtest_ordered_Outpatient
hyperglycemia	lung disease
lab_ANION GAP	med_dx_Acquired hypothyroidism
lab_ATRIAL RATE	med_dx_Anxiety
lab_BASOPHILS ABSOLUTE COUNT	med_dx_COVID-19
lab_BASOPHILS RELATIVE PERCENT	med_dx_Encounter for antineoplastic chemotherapy
lab_BLOOD UREA NITROGEN	med_dx_Encounter for antineoplastic chemotherapy and immunotherapy
lab_CALCIIUM	med_dx_Encounter for antineoplastic immunotherapy
lab_CALCUALTED T AXIS	med_dx_Encounter for immunization
lab_CALCULATED R AXIS	med_dx_Gastroesophageal reflux disease without esophagitis
lab_CHLORIDE	med_dx_Gastroesophageal reflux disease, esophagitis presence not specified
lab_CO2	med_dx_Generalized anxiety disorder
lab_CREATININE	med_dx_Hyperlipidemia, unspecified hyperlipidemia type
lab_EOSINOPHILS ABSOLUTE COUNT	med_dx_Hypomagnesemia
lab_EOSINOPHILS RELATIVE PERCENT	med_dx_Hypothyroidism, unspecified type
lab_GFR MDRD AF AMER	med_dx_Iron deficiency anemia, unspecified iron deficiency anemia type
lab_GFR MDRD NON AF AMER	med_dx_Mixed hyperlipidemia
lab_GLUKOSE	med_dx_Primary osteoarthritis of right knee
lab_IMMATURE GRANULOCYTES RELATIVE PERCENT	medication_ACETAMINOPHEN 325 MG TABLET
lab_LYMPHOCYTES ABSOLUTE COUNT	medication_ALBUTEROL SULFATE 2.5 MG/3 ML (0.083 % FOR NEBULIZATION)
lab_LYMPHOCYTES RELATIVE PERCENT	medication_ALBUTEROL SULFATE HFA 90 MCG/ACTUATION AEROSOL INHALER
lab_MEAN CORPUSCULAR HEMOGLOBIN	medication_ASPIRIN 81 MG TABLET, DELAYED RELEASE
lab_MEAN CORPUSCULAR HEMOGLOBIN CONC	medication_DEXAMETHASONE SODIUM PHOSPHATE 4 MG/ML INJECTION SOLUTION
	medication_DIPHENHYDRAMINE 50 MG/ML INJECTION (WRAPPER)
	medication_EPINEPHRINE 0.3 MG/0.3 ML INJECTION, AUTO-INJECTOR
	medication_FENTANYL (PF) 50 MCG/ML INJECTION SOLUTION

ZHOU CHEN LIPTON

medication_HYDROCODONE 5 MG-ACETAMINOPHEN 325 MG TABLET
medication_HYDROCORTISONE SOD SUCCINATE (PF) 100 MG/2 ML SOLUTION
FOR INJECTION
medication_IOPAMIDOL 76 %
medication_LACTATED RINGERS INTRAVENOUS SOLUTION
medication_MIDAZOLAM 1 MG/ML INJECTION SOLUTION
medication_NALOXONE 0.4 MG/ML INJECTION SOLUTION
medication_ONDANSETRON HCL (PF) 4 MG/2 ML INJECTION SOLUTION
medication_OXYCODONE 5 MG TABLET
medication_PANTOPRAZOLE 40 MG TABLET,DELAYED RELEASE
medication_PROPOFOL 10 MG/ML INTRAVENOUS BOLUS (20 ML)
medication_SODIUM CHLORIDE 0.9 %
medication_SODIUM CHLORIDE 0.9 %
myalgia
obesity
past7Dprobhx_ICD_Acute kidney failure, unspecified
past7Dprobhx_ICD_Anemia, unspecified
past7Dprobhx_ICD_Anxiety disorder, unspecified
past7Dprobhx_ICD_Chest pain, unspecified
past7Dprobhx_ICD_Dizziness and giddiness
past7Dprobhx_ICD_Encounter for general adult medical examination
without abnormal findings
past7Dprobhx_ICD_Encounter for immunization
past7Dprobhx_ICD_Encounter for screening for malignant
neoplasm of colon
past7Dprobhx_ICD_F32.A
past7Dprobhx_ICD_Gastro-esophageal reflux disease
without esophagitis
past7Dprobhx_ICD_Hyperlipidemia, unspecified
past7Dprobhx_ICD_Hypokalemia
past7Dprobhx_ICD_Hypothyroidism, unspecified
past7Dprobhx_ICD_Mixed hyperlipidemia
past7Dprobhx_ICD_Obstructive sleep apnea (adult) (pediatric)
past7Dprobhx_ICD_Syncope and collapse
past7Dprobhx_ICD_Type 2 diabetes mellitus without complications
past7Dprobhx_ICD_Unspecified atrial fibrillation
probhx_ICD_Acute kidney failure, unspecified
probhx_ICD_Anemia, unspecified
probhx_ICD_Anxiety disorder, unspecified
probhx_ICD_Chest pain, unspecified
probhx_ICD_Dizziness and giddiness
probhx_ICD_Encounter for general adult medical examination without
abnormal findings
probhx_ICD_Encounter for immunization
probhx_ICD_Encounter for screening for malignant neoplasm of colon
probhx_ICD_F32.A
probhx_ICD_Gastro-esophageal reflux disease without esophagitis
probhx_ICD_Hyperlipidemia, unspecified
probhx_ICD_Hypokalemia
probhx_ICD_Hypothyroidism, unspecified
probhx_ICD_Mixed hyperlipidemia
probhx_ICD_Obstructive sleep apnea (adult) (pediatric)
probhx_ICD_Syncope and collapse
probhx_ICD_Type 2 diabetes mellitus without complications
probhx_ICD_Unspecified atrial fibrillation
transplant
troponin
vaccine_COVID-19_RS-AD26 (PF) Vaccine (Janssen)
vaccine_COVID-19 Vaccine, Unspecified
vaccine_COVID-19 mRNA (PF) Vaccine (Moderna)
vaccine_COVID-19 mRNA (PF) Vaccine (Pfizer)
vaccine_Flu Whole
vaccine_INFLUENZA, CCIV4
vaccine_Influenza
vaccine_Influenza High PF
vaccine_Influenza ID PF
vaccine_Influenza PF
vaccine_Influenza Vaccine, Quadrivalent, Adjuvanted
vaccine_Influenza, High-dose, Quadrivalent
vaccine_Influenza, Quadrivalent
vaccine_Influenza, Recombinant (RIV4)
vaccine_Influenza, Recombinant (Riv3)
vaccine_Influenza, Trivalent, Adjuvanted
vaccine_LAIV3
vaccine_Pneumococcal
vaccine_Pneumococcal Conjugate 13-valent
vaccine_Pneumococcal Polysaccharide
vaccine_TIVA

D.3. Missingness heatmaps

This section plots missingness heatmaps of categorical and numerical features over time. Darker color means larger proportion of missing data.

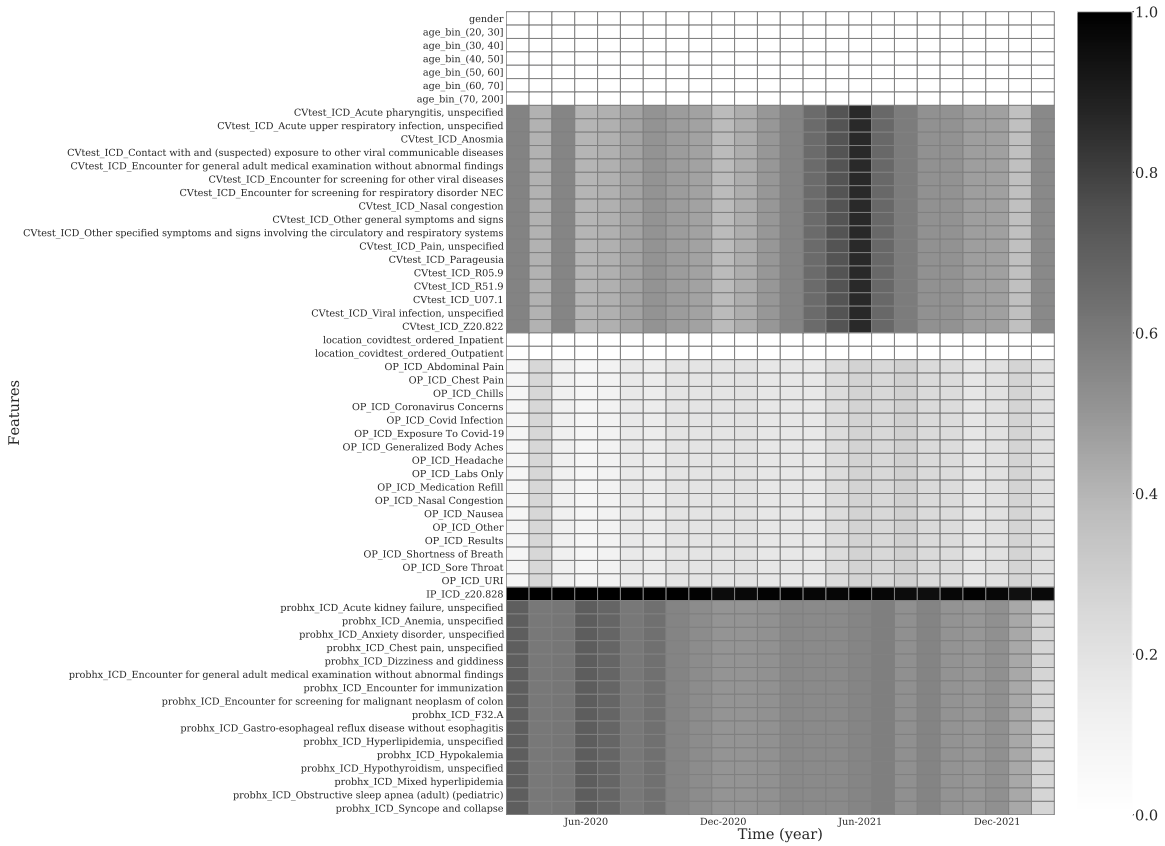


Figure 20: Missingness of categorical features in SWPA COVID-19 dataset (part 1).

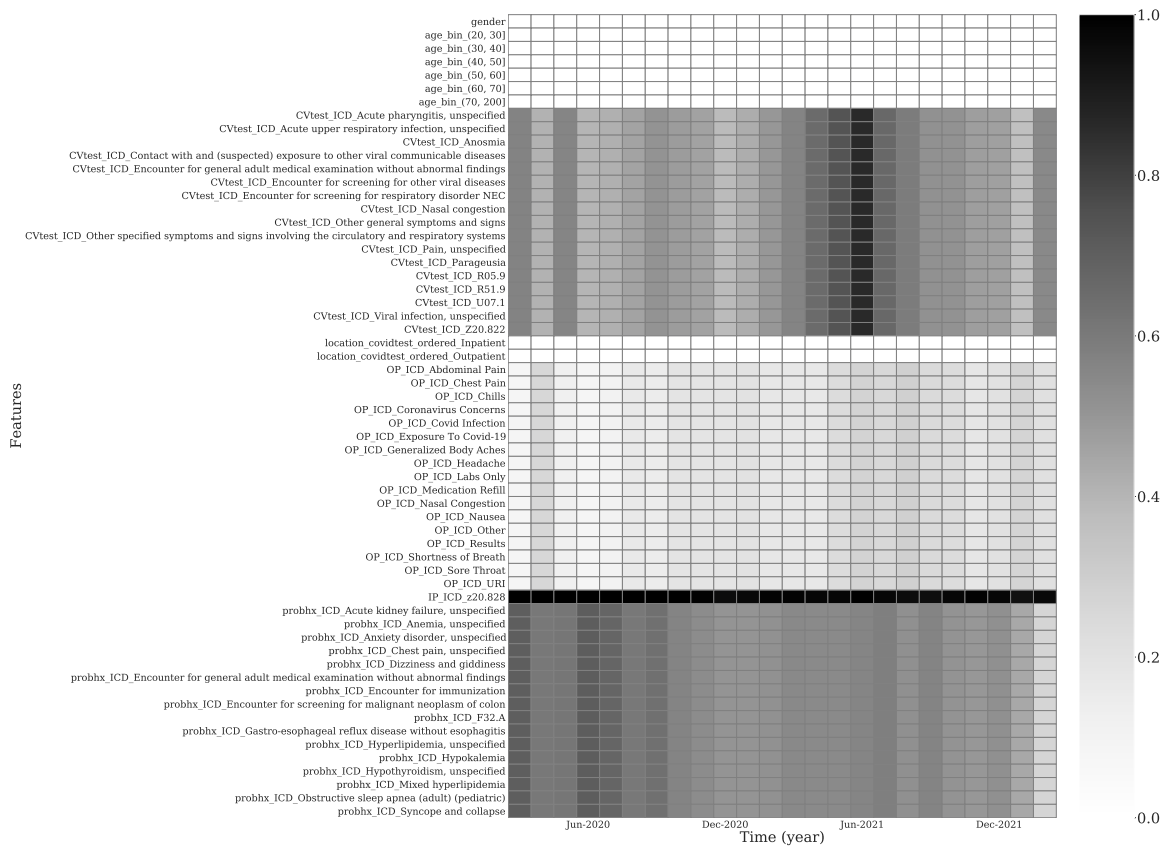


Figure 21: Missingness of categorical features in SWPA COVID-19 dataset (part 2).

MODEL EVALUATION IN MEDICAL DATASETS OVER TIME

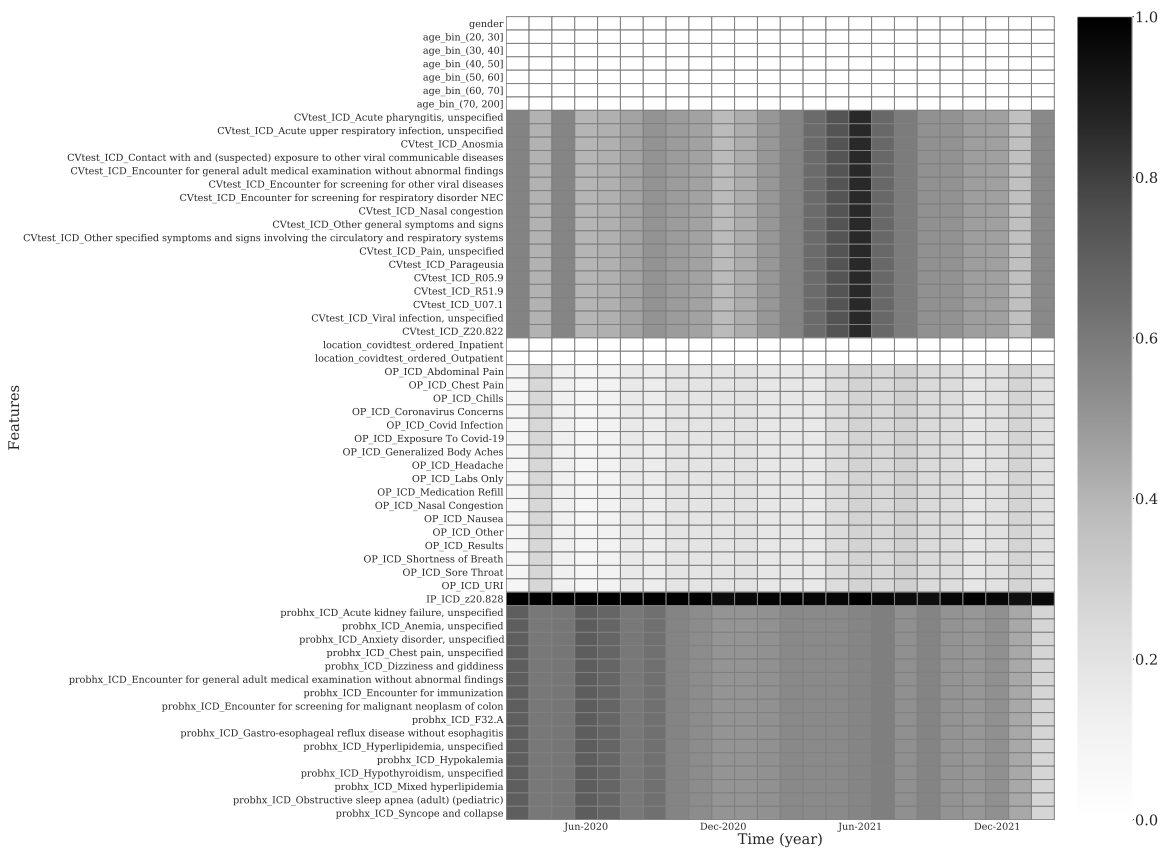


Figure 22: Missingness of categorical features in SWPA COVID-19 dataset (part 3).

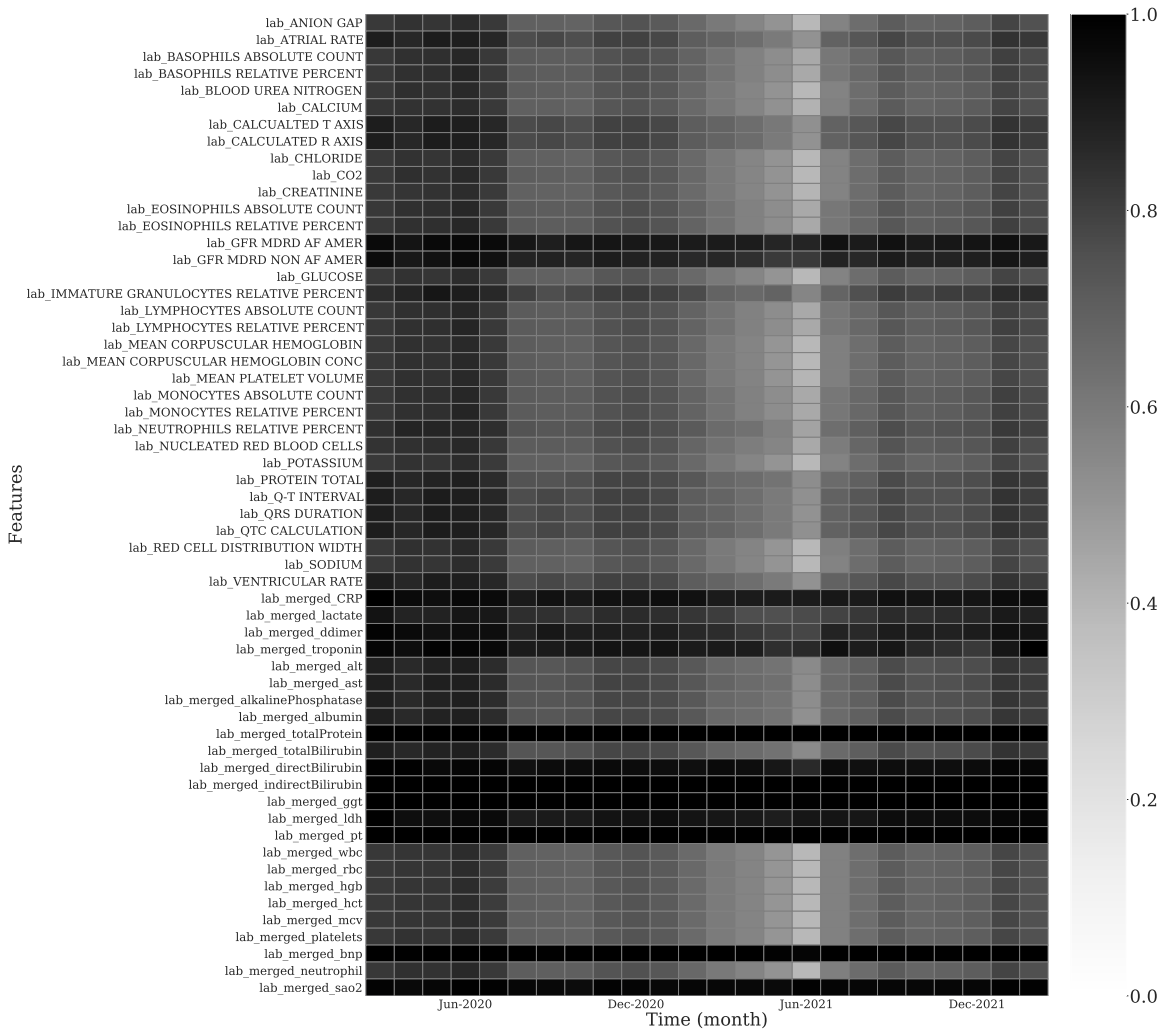


Figure 23: Missingness of numerical features in SWPA COVID-19.

Appendix E. Additional MIMIC-IV Data Details

The Medical Information Mart for Intensive Care (MIMIC)-IV (Johnson et al., 2021) database contains EHR data from patients admitted to critical care units from 2008–2019. MIMIC-IV is an update to MIMIC-III, adding time annotations placing each sample into a three-year time range, and removing elements from the old CareVue EHR system (before 2008). We approximate the year of each sample by taking the midpoint of its time range. The performance over time is evaluated on a *yearly* basis. Our study uses MIMIC-IV-1.0.

- Data access: Users must create a Physionet account, become credentialed, and sign a data use agreement (DUA).
- Cohort selection: We select all patients in the `icustays` table, filtering for their first encounter (minimum `intime`), and defining a feature vector only using information available by the first 24 hrs of their first encounter. (Selection diagram in Figure 24). If there are multiple samples per patient, we filter to the first entry per patient, which corresponds to when a patient first enters the dataset. This corresponds to a particular interpretation of the prediction: when a patient first visits the ICU, given what we know about that patient, what is their estimated risk of in-ICU mortality?
- Outcome definition: The outcome of interest is in-ICU mortality, defined by comparing the `outtime` of the patient’s ICU visit with the patient’s `dod` (date of death, in the `patients` table). As noted in the documentation, out-of-hospital mortality is not recorded.
- Cohort characteristics: Cohort characteristics are given in Table 8.
- Features: We list the features used in the MIMIC-IV datasets in Section E.2. We convert all categorical variables into dummy features, and apply standard scaling to numerical variables (subtract mean and divide by standard deviation). To create a fixed length feature vector, we take the most recent value of any patient history data available (e.g. most recent lab values).
- Missingness heat maps: are given in Figures 25, 26, 27, 28.

E.1. Cohort Selection and Cohort Characteristics

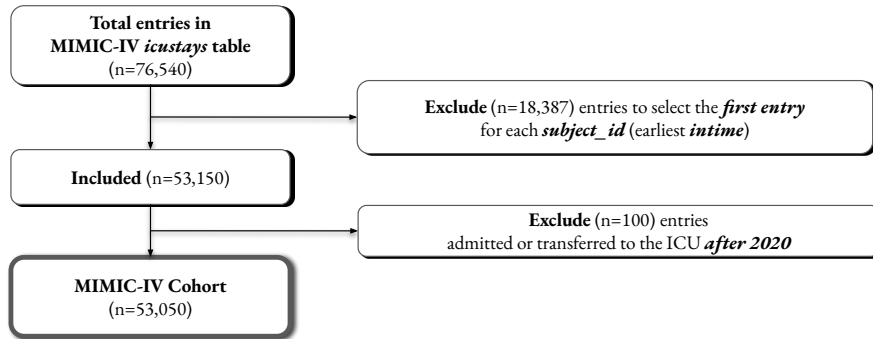


Figure 24: Cohort selection diagram - MIMIC-IV

Table 8: MIMIC-IV cohort characteristics, with count (%) or median (Q1–Q3).

Characteristic		Missingness	Type
Gender			
Female	23,313 (43.9%)	–	categorical
Male	29,737 (56.1%)	–	categorical
Age at Admission	66 (54-78)	0.0%	continuous
O2 Delivery Device(s)			
Use device	33,359 (62.9%)	–	categorical
None	18,549 (35.0%)	–	categorical
Missing	1,142 (2.2%)	–	categorical
Pupil Response R			
Brisk	39,708 (74.9%)	–	categorical
Sluggish	4,603 (8.7%)	–	categorical
Non-reactive	1,812 (3.4%)	–	categorical
Missing	6,927 (13.1%)	–	categorical
first_careunit			
Medical Intensive Care Unit (MICU)	10,213 (19.3%)	–	categorical
Surgical Intensive Care Unit (SICU)	8,241 (15.5%)	–	categorical
Medical/Surgical Intensive Care Unit (MICU/S...	8,808 (16.6%)	–	categorical
Cardiac Vascular Intensive Care Unit (CVICU)	9,437 (17.8%)	–	categorical
Coronary Care Unit (CCU)	6,098 (11.5%)	–	categorical
Trauma SICU (TSICU)	6,947 (13.1%)	–	categorical
Other	3,306 (6.2%)	–	categorical
Anion Gap	13 (11-16)	0.5%	continuous
Heart Rhythm			
SR (Sinus Rhythm)	34,004 (64.1%)	–	categorical
Abnormal heart rhythm	18,657 (35.2%)	–	categorical
Missing	389 (0.7%)	–	categorical
Glucose FS (range 70 -100)	131 (110-164)	32.7%	continuous
Eye Opening			
Spontaneously	39,216 (73.9%)	–	categorical
To Speech	7,387 (13.9%)	–	categorical
None	4,538 (8.6%)	–	categorical
To Pain	1,702 (3.2%)	–	categorical
Missing	207 (0.4%)	–	categorical
Lactate	2 (1-2)	22.0%	continuous
Motor Response			
Obeys Commands	44,409 (83.7%)	–	categorical
Localizes Pain	3,419 (6.4%)	–	categorical
Flex-withdraws	1,673 (3.2%)	–	categorical
No response	2,930 (5.5%)	–	categorical
Abnormal extension	157 (0.3%)	–	categorical
Abnormal Flexion	238 (0.4%)	–	categorical
Missing	224 (0.4%)	–	categorical
Respiratory Pattern			
Regular	29,373 (55.4%)	–	categorical
Not regular	1,739 (3.3%)	–	categorical
Missing	21,938 (41.4%)	–	categorical
Richmond-RAS Scale	0 (-1-0)	15.4%	categorical
in-icu mortality			
0	49,716 (93.7%)	–	categorical
1	3,334 (6.3%)	–	categorical

E.2. Features

18 Gauge Dressing Occlusive
 18 Gauge placed in outside facility
 20 Gauge Dressing Occlusive
 20 Gauge placed in outside facility
 20 Gauge placed in the field
 Abdominal Assessment
 Activity
 Activity Tolerance
 Admission Weight (Kg)
 Admission Weight (lbs.)
 Alanine Aminotransferase (ALT)
 Alarms On
 Albumin
 Alkaline Phosphatase
 All Medications Tolerated
 Ambulatory aid
 Anion Gap
 Anion gap
 Anti Embolic Device
 Anti Embolic Device Status
 Asparate Aminotransferase (AST)
 Assistance
 BUN
 Balance
 Base Excess
 Basophils
 Bath
 Bicarbonate
 Bilirubin, Total
 Bowel Sounds
 Braden Activity
 Braden Friction/Shear
 Braden Mobility
 Braden Moisture
 Braden Nutrition
 Braden Sensory Perception
 CAM-ICU MS Change
 Calcium non-ionized
 Calcium, Total
 Calculated Total CO2
 Capillary Refill L
 Capillary Refill R
 Chloride
 Chloride (serum)
 Commands
 Commands Response
 Cough Effort
 Cough Type
 Creatinine
 Creatinine (serum)
 Currently experiencing pain
 Daily Wake Up
 Delirium assessment
 Dialysis patient
 Diet Type
 Difficulty swallowing
 Dorsal PedPulse L
 Dorsal PedPulse R
 ETOH
 Ectopy Type 1
 Edema Amount
 Edema Location
 Education Barrier
 Education Existing Knowledge
 Education Learner
 Education Method
 Education Readiness/Motivation
 Education Response
 Education Topic
 Eosinophils
 Epithelial Cells
 Eye Opening
 Family Communication
 Flatus
 GU Catheter Size
 Gait/Transferring
 Glucose (serum)
 Glucose FS (range 70 -100)
 Goal Richmond-RAS Scale
 HCO3 (serum)
 HOB
 HR
 HR Alarm - High
 HR Alarm - Low
 Heart Rhythm
 Height
 Height (cm)
 Hematocrit
 Hematocrit (serum)
 Hemoglobin
 History of falling (within 3 mnths)*
 History of slips / falls
 Home TF
 INR
 INR(PT)
 IV/Saline lock
 Insulin pump
 Intravenous / IV access prior to admission
 Judgement
 LLE Color
 LLE Temp
 LLL Lung Sounds
 LUE Color
 LUE Temp
 LUL Lung Sounds
 Lactate
 Lactic Acid
 Living situation
 Lymphocytes
 MCH
 MCHC
 MCV
 Magnesium
 Mental status
 Monocytes
 Motor Response
 NBP Alarm - High
 NBP Alarm - Low
 NBP Alarm Source
 NBPd
 NBPm
 NBPs
 Nares L
 Nares R
 Neutrophils
 O2 Delivery Device(s)
 Oral Care
 Oral Cavity
 Orientation
 PT
 PTT
 Pain Assessment Method
 Pain Cause
 Pain Level
 Pain Level Acceptable
 Pain Level Response
 Pain Location
 Pain Management
 Pain Present
 Pain Type
 Parameters Checked
 Phosphate
 Phosphorous
 Platelet Count
 Position
 PostTib Pulses L
 PostTib Pulses R
 Potassium
 Potassium (serum)
 Potassium, Whole Blood
 Pressure Reducing Device
 Pressure Ulcer Present
 Pupil Response L
 Pupil Response R
 Pupil Size Left
 Pupil Size Right
 RBC
 RDW
 RLE Color
 RLE Temp
 RLL Lung Sounds
 RR
 RUE Color
 RUE Temp
 RUL Lung Sounds
 Radial Pulse L
 Radial Pulse R
 Red Blood Cells
 Resp Alarm - High
 Resp Alarm - Low
 Respiratory Effort
 Respiratory Pattern

MODEL EVALUATION IN MEDICAL DATASETS OVER TIME

Richmond-RAS Scale
ST Segment Monitoring On
Safety Measures
Secondary diagnosis
Self ADL
Side Rails
Skin Color
Skin Condition
Skin Integrity
Skin Temp
Sodium
Sodium (serum)
SpO2
SpO2 Alarm - High
SpO2 Alarm - Low
SpO2 Desat Limit
Specific Gravity
Specimen Type
Speech
Strength L Arm
Strength L Leg
Strength R Arm
Strength R Leg
Support Systems
Temp Site
Temperature F
Therapeutic Bed
Tobacco Use History
Turn
Untoward Effect
Urea Nitrogen
Urine Source
Verbal Response
Visual / hearing deficit
WBC
White Blood Cells
Yeast
admit_age
gender
pCO2
pH
pO2

E.3. Missingness heatmaps

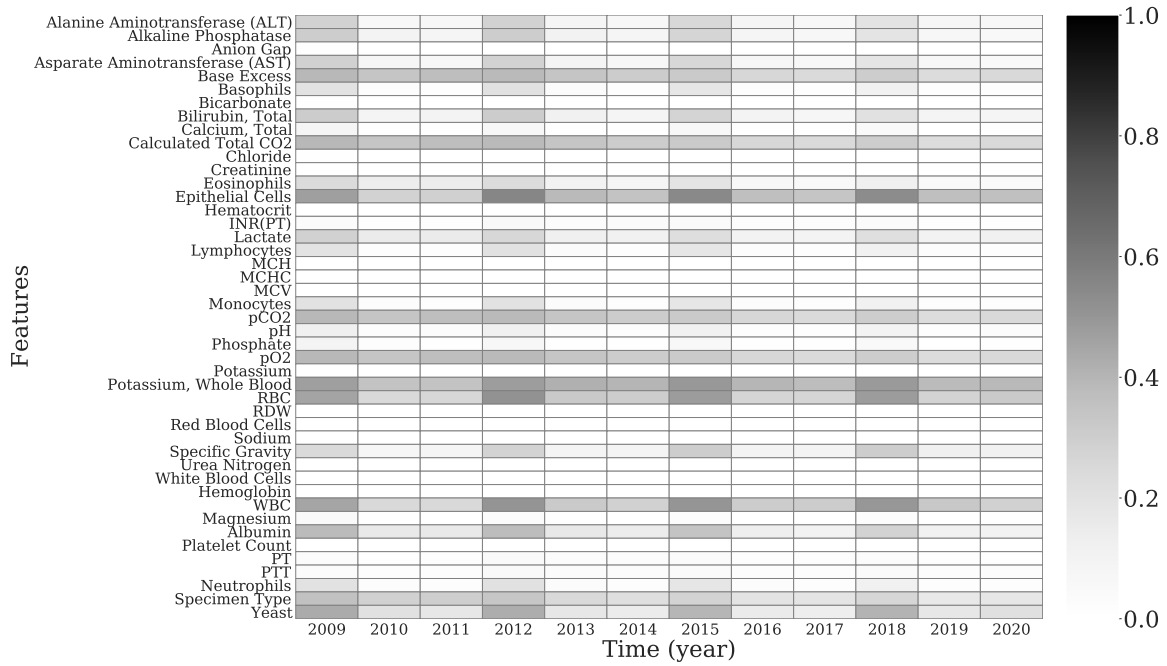


Figure 25: Missingness over time for labevents features in MIMIC-IV dataset after cohort selection. The darker the color, the larger the proportion of missing data.

MODEL EVALUATION IN MEDICAL DATASETS OVER TIME

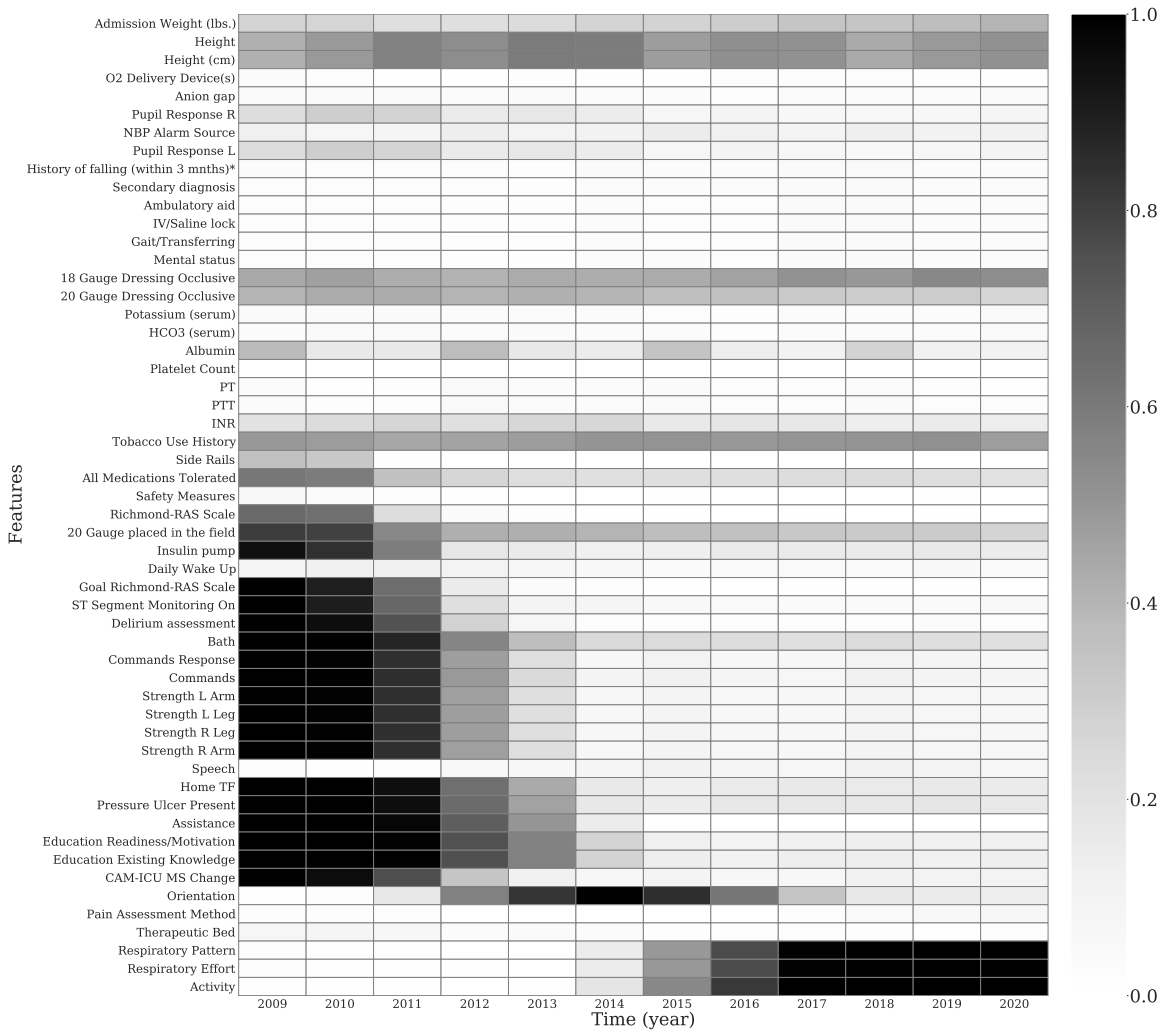


Figure 26: Missingness over time for chartevents features in MIMIC-IV dataset after cohort selection. The darker the color, the larger the proportion of missing data. (part 1)

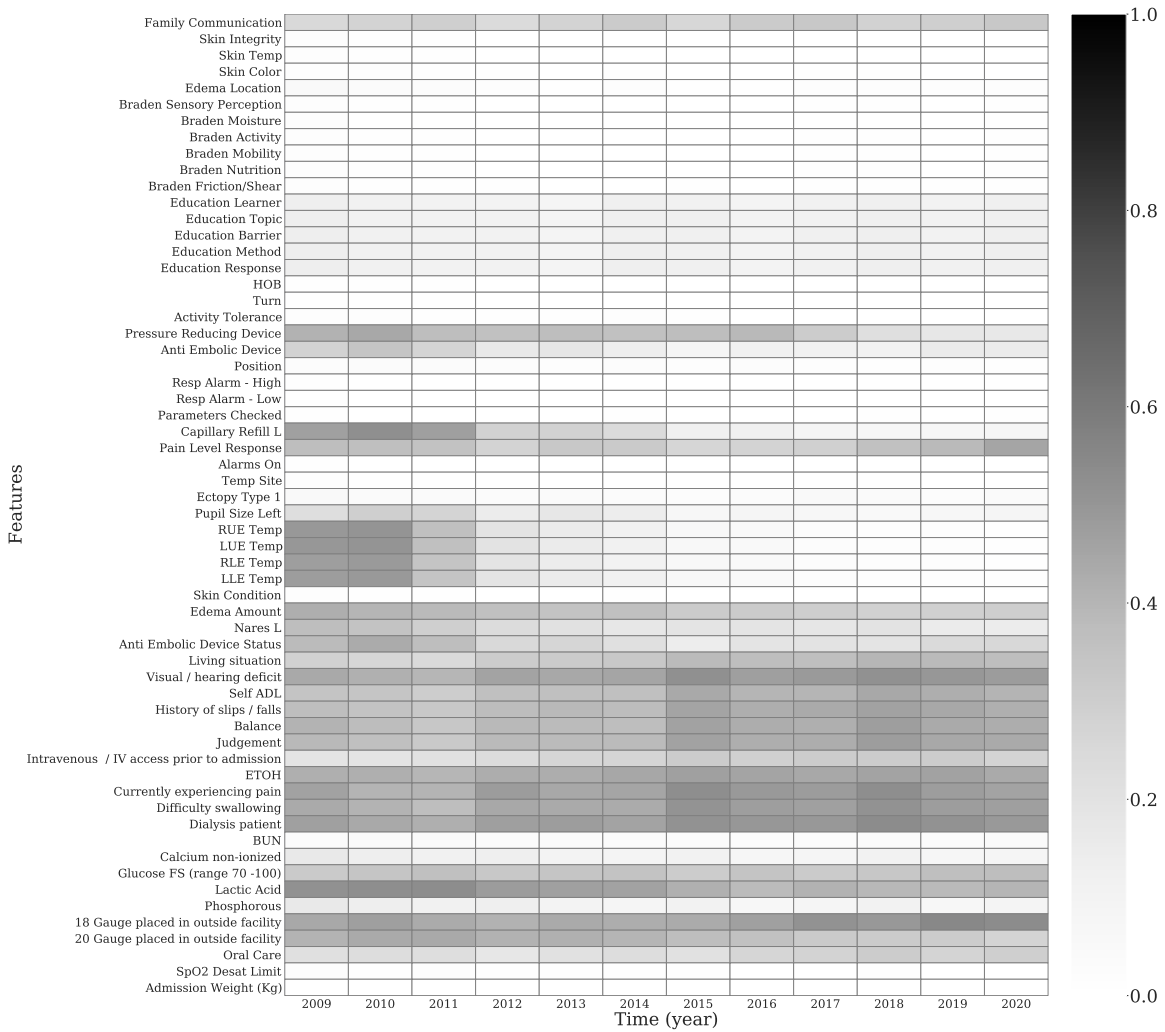


Figure 27: Missingness over time for chartevents features in MIMIC-IV dataset after cohort selection. The darker the color, the larger the proportion of missing data. (part 2)

MODEL EVALUATION IN MEDICAL DATASETS OVER TIME

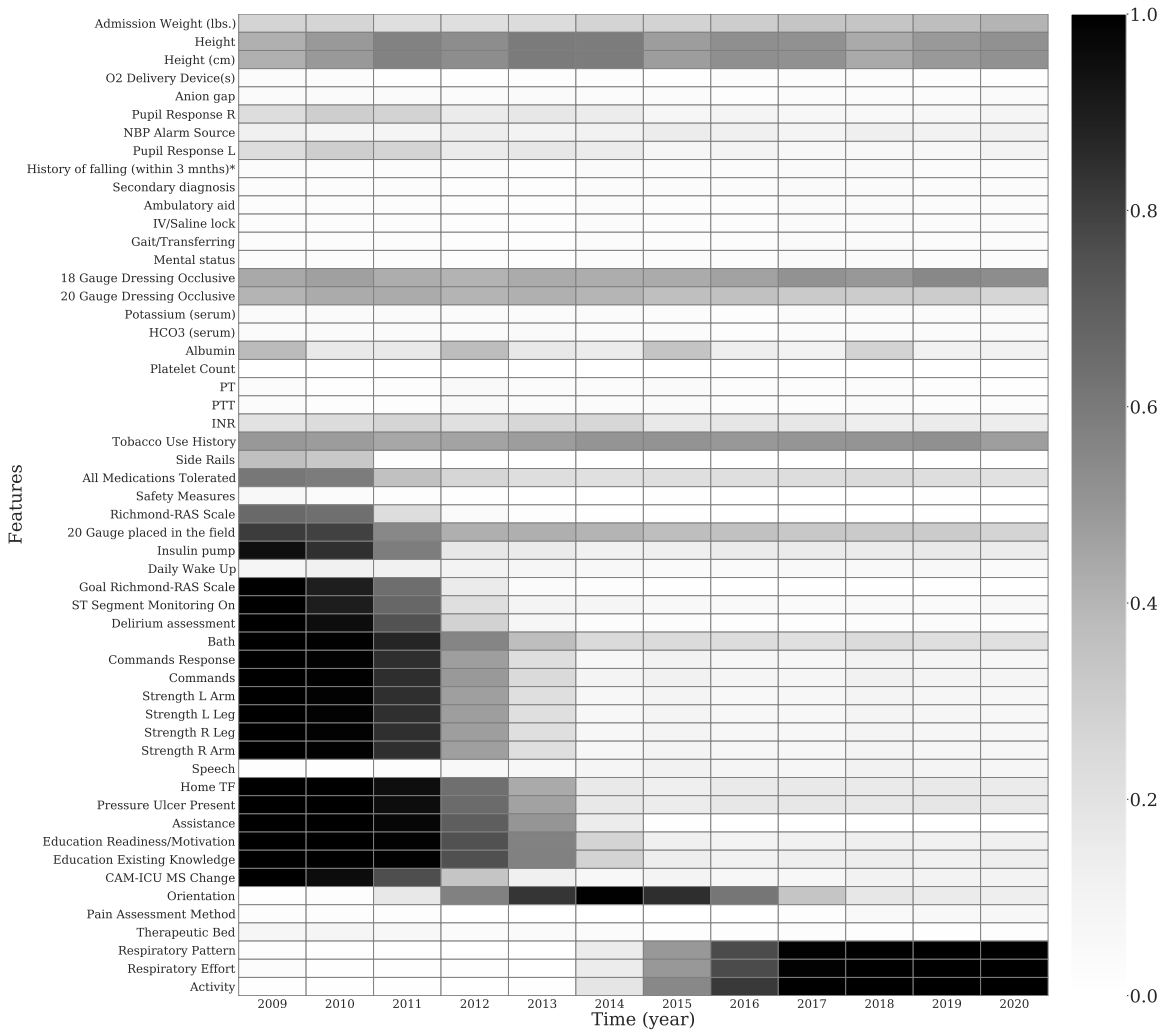


Figure 28: Missingness over time for chartevents features in MIMIC-IV dataset after cohort selection. The darker the color, the larger the proportion of missing data. (part 3)

Appendix F. Additional OPTN (Liver) Data Details

The Organ Procurement and Transplantation Network (OPTN) database tracks organ donation and transplant events in the U.S. Our study uses data from candidates on the liver transplant wait list. The performance over time is evaluated on a *yearly* basis.

- First, we provide the disclaimer: “The data reported here have been supplied by the United Network for Organ Sharing as the contractor for the Organ Procurement and transplantation Network. The interpretation and reporting of these data are the responsibility of the author(s) and in no way should be seen as an official policy of or interpretation by the OPTN or the U.S. Government”.
- Data access: After signing the Data Use Agreement - I from Organ Procurement And Transplantation network, users can access the OPTN (Liver) dataset.
- Cohort selection: The cohort consists of liver transplant candidates on the waiting list (2005-2017). We follow the same pipeline as [Byrd et al. \(2021\)](#) to extract the data, except that we select the first record for each patient. Cohort selection diagrams are given in [Figures 29](#). This corresponds to a particular interpretation of the prediction: when a patient is first added to the transplant list, given what we know about that patient, what is their estimated risk of 180-day mortality?
- Outcome definition: 180-day mortality from when the patient was first added to the list
- Cohort characteristics: Cohort characteristics are given in [Table 9](#).
- Features: We list the features used in the OPTN liver dataset in [Section F.2](#). We convert all categorical variables into dummy features, and apply standard scaling to numerical variables (subtract mean and divide by standard deviation).
- Missingness heat maps: are given in [Figures 30](#) and [31](#).

F.1. Cohort Selection and Cohort Characteristics

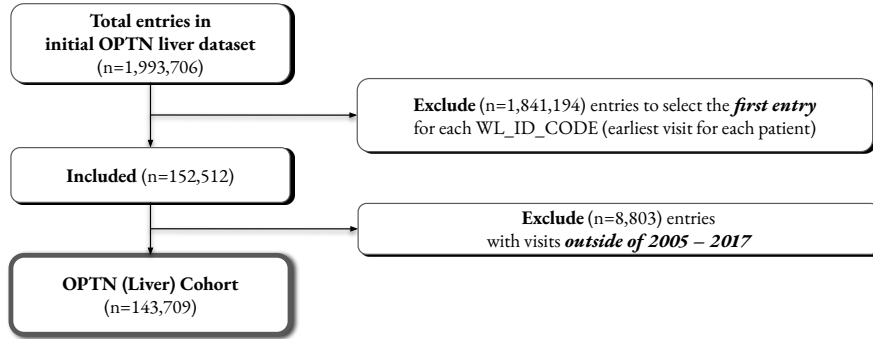


Figure 29: Cohort selection diagram - OPTN (Liver)

Table 9: OPTN (Liver) cohort characteristics, with count (%) or median (Q1 – Q3).

Feature name (value)		Empty (ratio)	Type
Gender			
Male	92,560 (64.4%)	–	categorical
Female	51,149 (35.6%)	–	categorical
INIT_AGE	56 (49-62)	0.0%	continuous
FUNC_STAT_TCR	2,070 (2,050-2,080)	0.0%	categorical
INIT_OPO_CTR_CODE	11,036 (3,782-19,282)	0.0%	categorical
ALBUMIN	3 (3-4)	0.0%	continuous
HCC_DIAGNOSIS_TCR			
No	31,390 (21.8%)	–	categorical
Yes	11,312 (7.9%)	–	categorical
Missing	101,007 (70.3%)	–	categorical
PERM_STATE			
CA	19,645 (13.7%)	–	categorical
TX	14,692 (10.2%)	–	categorical
NY	9,976 (6.9%)	–	categorical
GA	4,052 (2.8%)	–	categorical
MD	4,050 (2.8%)	–	categorical
FL	7,602 (5.3%)	–	categorical
PA	8,013 (5.6%)	–	categorical
MI	3,989 (2.8%)	–	categorical
Other	71,007 (49.4%)	–	categorical
EDUCATION	4 (3-5)	0.0%	categorical
ASCITES	2 (1-2)	0.0%	categorical
MORTALITY_180D			
1	4,635 (3.2%)	–	categorical
0	139,074 (96.8%)	–	categorical

F.2. Features

ABO
 BACT_PERIT_TCR
 CITIZENSHIP
 DGN_TCR
 DGN2_TCR
 DIAB
 EDUCATION
 FUNC_STAT_TCR
 GENDER
 LIFE_SUP_TCR
 MALIG_TCR
 OTH_LIFE_SUP_TCR
 PERM_STATE
 PORTAL_VEIN_TCR
 PREV_AB_SURG_TCR
 PRI_PAYMENT_TCR
 REGION
 TIPSS_TCR
 VENTILATOR_TCR
 WORK_INCOME_TCR
 ETHCAT
 HCC_DIAGNOSIS_TCR
 MUSCLE_WAST_TCR
 INIT_OPO_CTR_CODE
 WLHR
 WLIN
 WLKI
 WLLU
 WLPA
 INACTIVE
 ASCITES
 ENCEPH
 DIALYSIS_PRIOR_WEEK
 INIT_HGT_CM
 INIT_WGT_KG
 INIT_BMI_CALC
 INIT_AGE
 UNOS_CAND_STAT_CD
 BILIRUBIN
 SERUM_CREAT
 INR
 SERUM_SODIUM
 ALBUMIN
 BILIRUBIN_DELTA
 SERUM_CREAT_DELTA
 INR_DELTA
 SERUM_SODIUM_DELTA
 ALBUMIN_DELTA

F.3. Missingness heatmaps

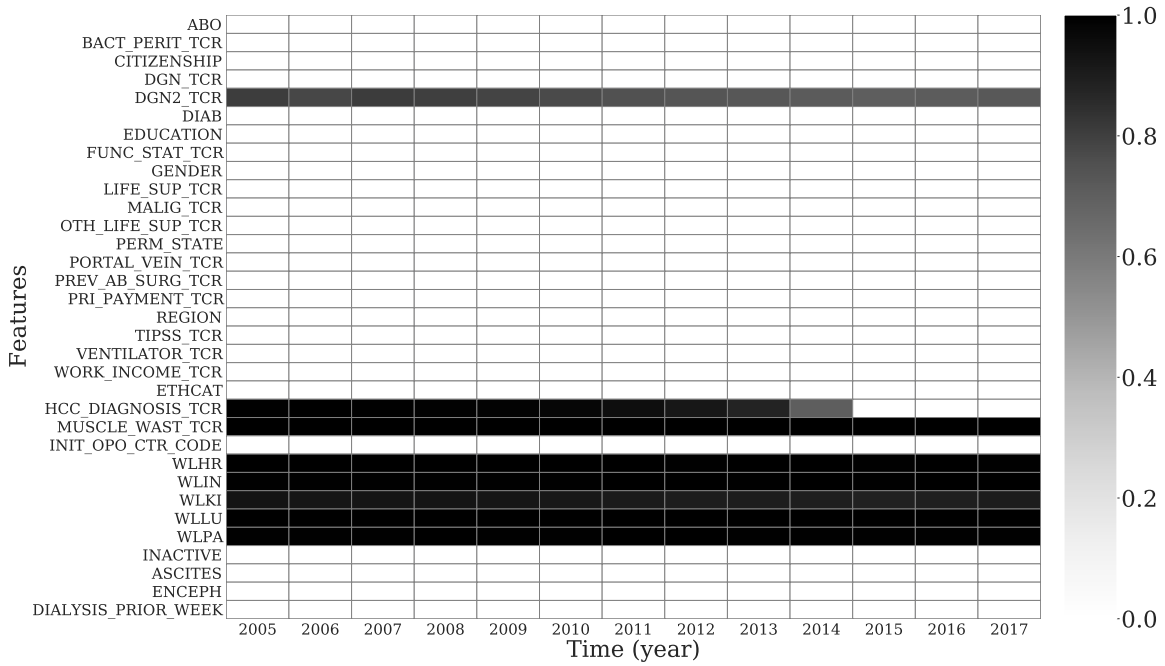


Figure 30: Missingness over time for categorical features in OPTN (Liver) dataset after cohort selection. The darker the color, the larger the proportion of missing data.

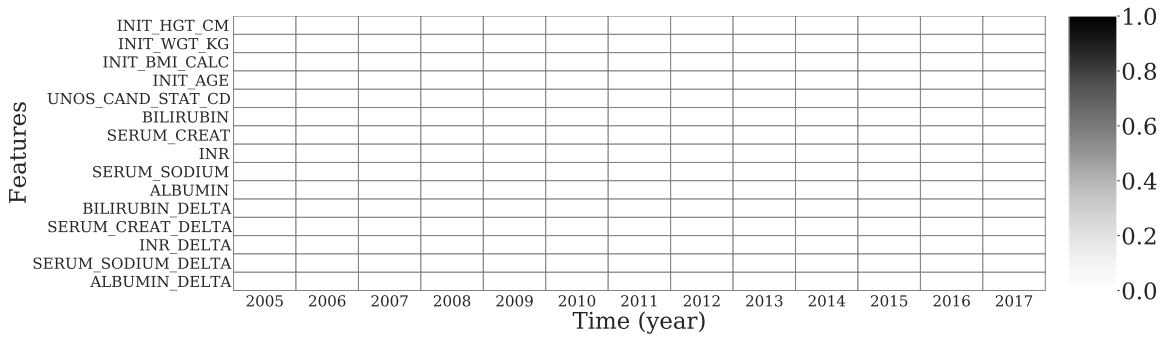


Figure 31: Missingness over time for numerical features in OPTN (Liver) dataset after cohort selection. The darker the color, the larger the proportion of missing data. (Near-zero missingness here.)

Appendix G. Logistic Regression Coefficients from Splitting by Patient

To help with intuition in important features for the predictive task on each dataset, here we have the coefficients of logistic regression models trained from splitting by patient.

Table 10: SEER (Breast) top 10 important features for LR models, all-period training.

Feature	Coefficient
SEER historic stage A (1973-2015)_Distant	-2.113944
SEER historic stage A (1973-2015)_Localized	1.676493
Regional nodes examined (1988+)_95.0	-1.167844
CS lymph nodes (2004-2015)_750	1.100824
CS lymph nodes (2004-2015)_755	1.023753
Histologic Type ICD-O-3_8530	-0.913494
Histologic Type ICD-O-3_8543	0.902798
Breast - Adjusted AJCC 6th T (1988-2015)_T4d	0.899491
Histologic Type ICD-O-3_8211	0.877848
EOD 10 - extent (1988-2003)_85	-0.791136

Table 11: SEER (Colon) top 10 important features for LR models, all-period training.

Feature	Coefficient
Reason no cancer-directed surgery_Surgery performed	2.360161
Regional nodes positive (1988+)_00	1.897706
Regional nodes positive (1988+)_01	1.872008
modified AJCC stage 3rd (1988-2003)_40	-1.787481
EOD 10 - extent (1988-2003)_13	1.766066
Reason no cancer-directed surgery_Not recommended, contraindicated due to other cond; autopsy only (1973-2002)	-1.752474
EOD 10 - extent (1988-2003)_85	-1.732619
EOD 10 - extent (1988-2003)_70	-1.704333
CS mets at dx (2004-2015)_99	1.619905
CS mets at dx (2004-2015)_00	1.609454

Table 12: SEER (Lung) top 10 important features for LR models, all-period training.

Feature	Coefficient
Histologic Type ICD-O-3_8240	2.514539
EOD 4 - nodes (1983-1987)_0	2.074730
EOD 4 - nodes (1983-1987)_7	-1.777530
EOD 10 - size (1988-2003)_140	-1.587893
Histologic Type ICD-O-3_8141	-1.546566
CS tumor size (2004-2015)_998.0	-1.515856
EOD 4 - nodes (1983-1987)_6	-1.497022
Type of Reporting Source_Nursing/convalescent home/hospice	-1.338998
CS mets at dx (2004-2015)_51	-1.326595
EOD 10 - size (1988-2003)_150	-1.326196

Table 13: CDC COVID-19 top 10 important features for LR models, all-period training.

Feature	Coefficient
res_state_DE	2.202055
age_group_0 - 9 Years	-2.114818
age_group_80+ Years	1.965279
age_group_10 - 19 Years	-1.681099
res_state_GA	1.391469
age_group_70 - 79 Years	1.379589
res_county_WICHITA	1.290644
age_group_20 - 29 Years	-1.189734
res_county_SUMNER	-1.135073
mechvent_yn_Yes	1.117372

Table 14: SWPA COVID-19 top 10 important features for LR models according to experiments splitting by patient.

Feature	Coefficient
age_bin_(70, 200]_0	-0.781337
age_bin_(70, 200]_1	0.780673
medication_FENTANYL (PF) 50 MCG/ML INJECTION SOLUTION_0.0	0.651419
medication_EPINEPHRINE 0.3 MG/0.3 ML INJECTION, AUTO-INJECTOR_nan	-0.627565
medication_HYDROCORTISONE SOD SUCCINATE (PF) 100 MG/2 ML SOLUTION FOR INJECTION_0.0	0.544222
medication_HYDROCODONE 5 MG-ACETAMINOPHEN 325 MG TABLET_nan	-0.520368
medication_DEXAMETHASONE SODIUM PHOSPHATE 4 MG/ML INJECTION SOLUTION_0.0	0.502954
medication_ASPIRIN 81 MG TABLET,DELAYED RELEASE_nan	-0.479100
bmi_nan	-0.427569
age_bin_(60, 70]_0	-0.380688

Table 15: MIMIC-IV top 10 important features for LR models, all-period training.

Feature	Coefficient
O2 Delivery Device(s)_None	-0.307334
Eye Opening_None	0.301737
admit_age	0.299712
O2 Delivery Device(s)_Nasal cannula	-0.248463
Motor Response_Obeys Commands	-0.230931
Pupil Response L_Non-reactive	0.223776
Richmond-RAS Scale_ 0 Alert and calm	-0.205476
Temp Site_Blood	-0.204514
HR_0.0	0.197299
Diet Type_NPO	0.195156

Table 16: OPTN (Liver) top 10 important features for LR models, all-period training.

Feature	Coefficient
SERUM_CREAT_DELTA	0.660589
FUNC_STAT_TCR_2020.0	0.241507
FUNC_STAT_TCR_2080.0	-0.236288
DGNC_4110.0	-0.234680
REGION_5.0	0.223940
EDUCATION_998.0	0.218549
ASCITES_3.0	0.218329
ASCITES_1.0	-0.214076
INIT_OPO_CTR_CODE_1054	-0.209265
INIT_OPO_CTR_CODE_4743	-0.207778

Appendix H. Diagnostic plots

We select important features to highlight based on high positive proportions and high relative feature importance.

H.1. SEER (Breast)

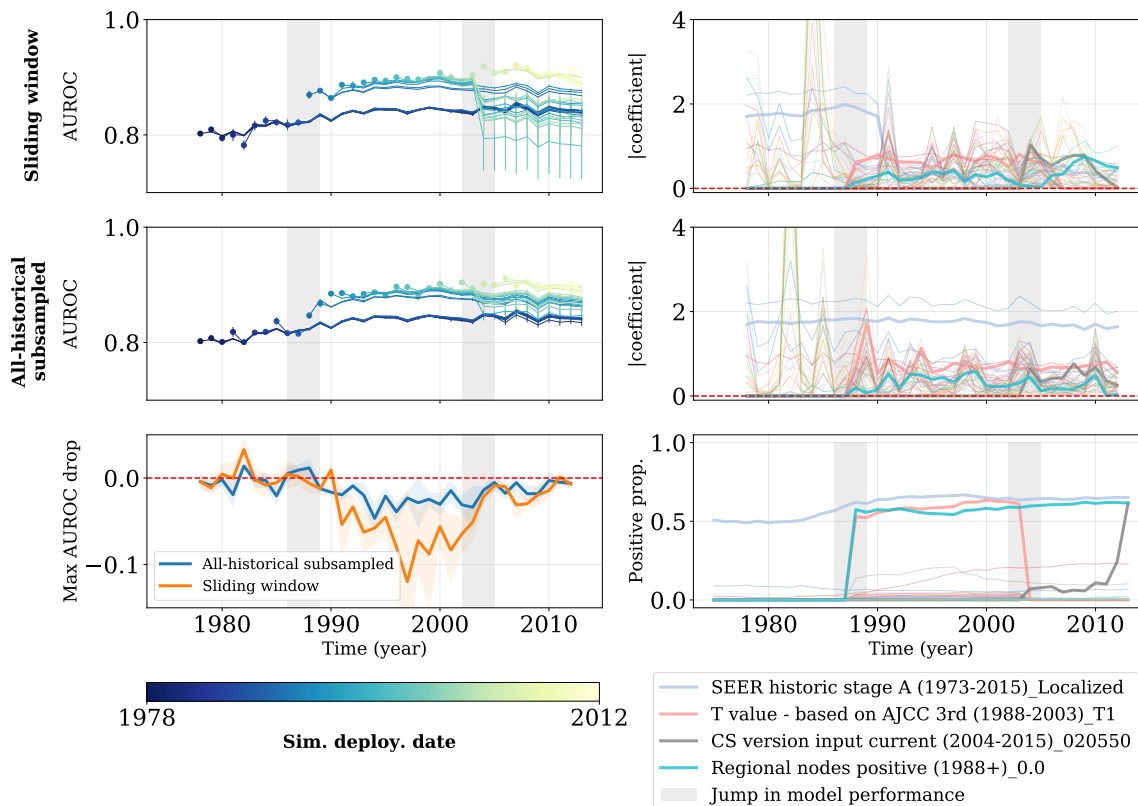


Figure 32: Diagnostic plot of SEER (Breast) dataset. The left column includes absolute AUROC versus time for both sliding window and all-historical subsampled, and the maximum AUROC drop for each trained model. The right column provides the absolute coefficients of each trained model from both regimes, and positive proportion of the significant features over time. As shown in the gray highlighted region, there are jumps in performance around 1988 and 2003, which coincides with the introducing and removal of several features (e.g. T value - based on AJCC 3rd (1988-2003)_T1). The latency of jumps in coefficients are caused by length of sliding window.

H.2. SEER (Colon)

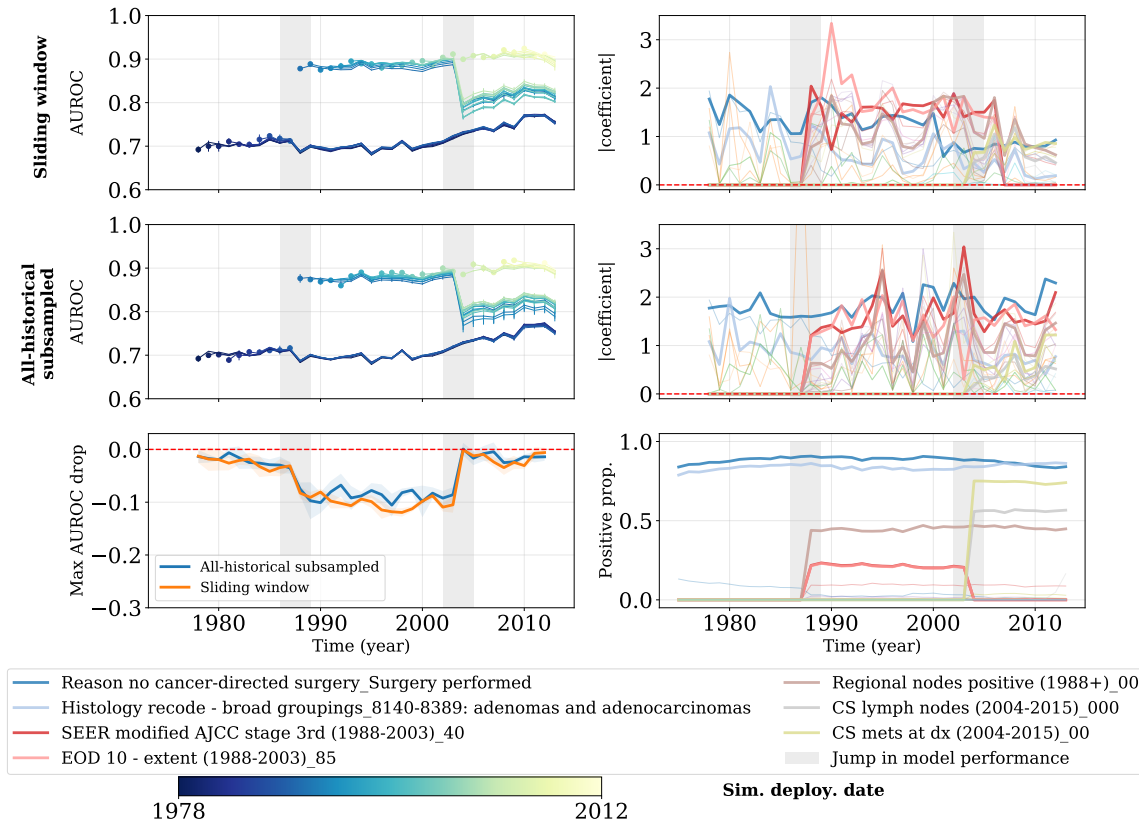


Figure 33: Diagnostic plot of SEER (Colon) dataset. The left column includes absolute AUROC versus time for both sliding window and all-historical subsampled, and the maximum AUROC drop for each trained model. The right column provides the absolute coefficients of each trained model from both regimes, and positive proportion of the significant features over time. As shown in the gray highlighted region, there are jumps in performance around 1988 and 2003, which coincides with the introducing and removal of several features (e.g. SEER modified AJCC stage 3rd (1988-2003)_40). The latency of jumps in coefficients are caused by length of sliding window.

H.3. SEER (Lung)

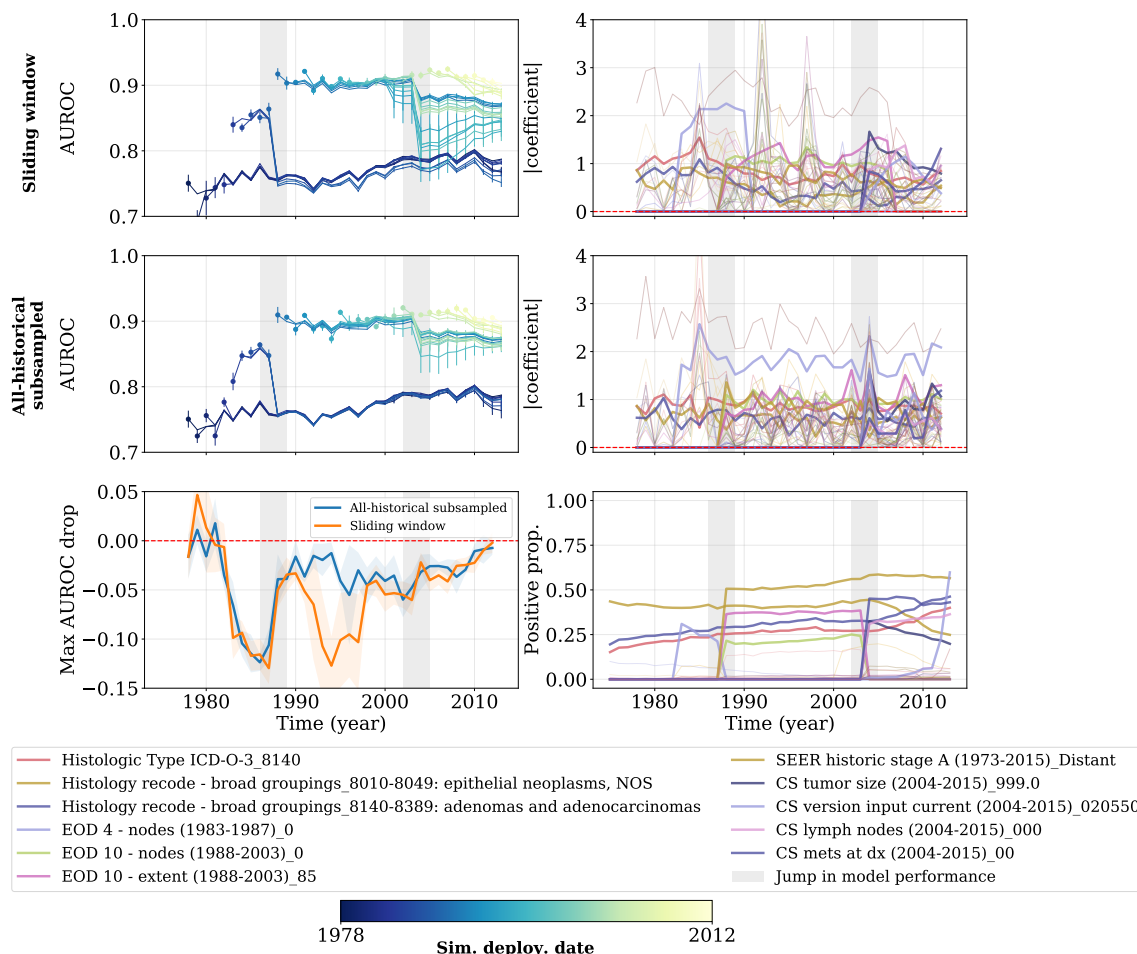


Figure 34: Diagnostic plot of SEER (Lung) dataset. The left column includes absolute AUROC versus time for both sliding window and all-historical subsampled, and the maximum AUROC drop for each trained model. The right column provides the absolute coefficients of each trained model from both regimes, and positive proportion of the significant features over time. As shown in the gray highlighted region, there are jumps in performance around 1988 and 2003, which coincides with the introducing and removal of several features (e.g. EOD 10 - nodes (1988-2013)_0 & EOD 10 - extent (1988-2003)_85). The latency of jumps in coefficients are caused by length of sliding window.

H.4. CDC COVID-19

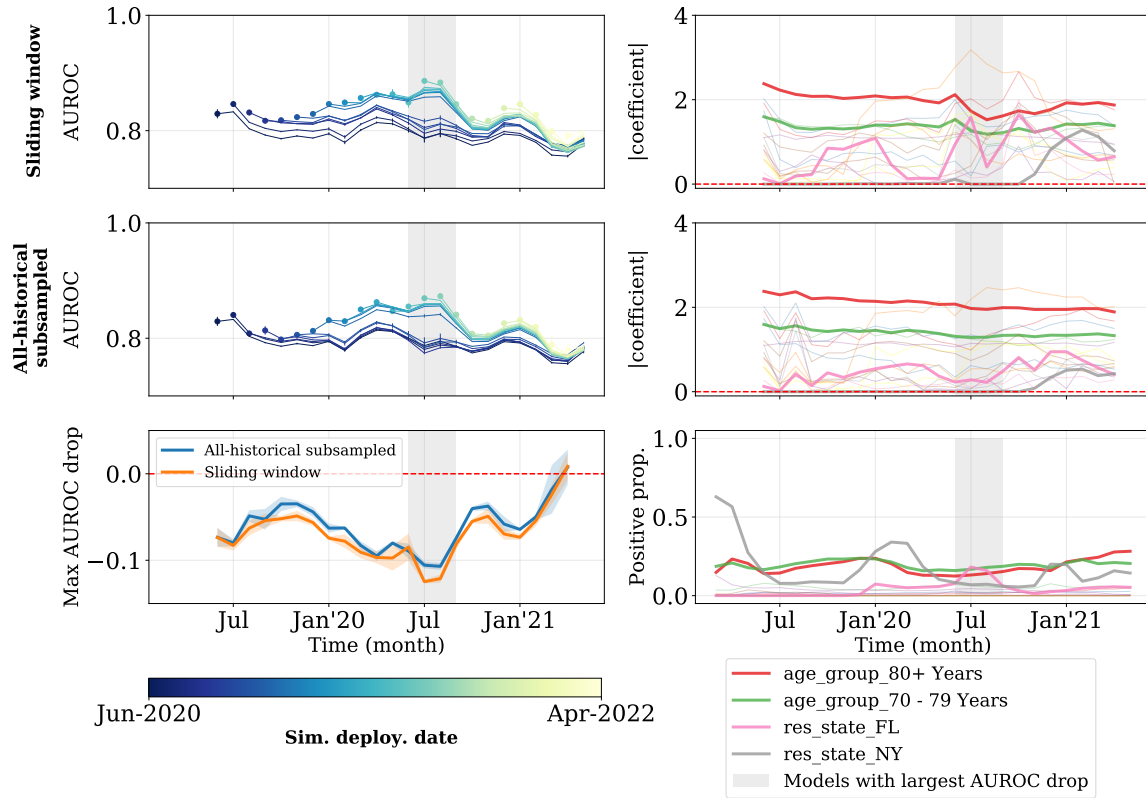


Figure 35: Diagnostic plot of CDC COVID-19. The left column includes absolute AUROC versus time for both sliding window and all-historical subsampled, and the maximum AUROC drop for each trained model. The right column provides the absolute coefficients of each trained model from both regimes, and positive proportion of the significant features over time. As shown in the gray highlighted region, the models trained around June 2021 suffer the largest maximum AUROC drop, coinciding with a shift in distribution of ages (Figure 18(a)) and states (Figure 18(b)). The latency of jumps in coefficients are caused by length of sliding window.

H.5. SWPA COVID-19

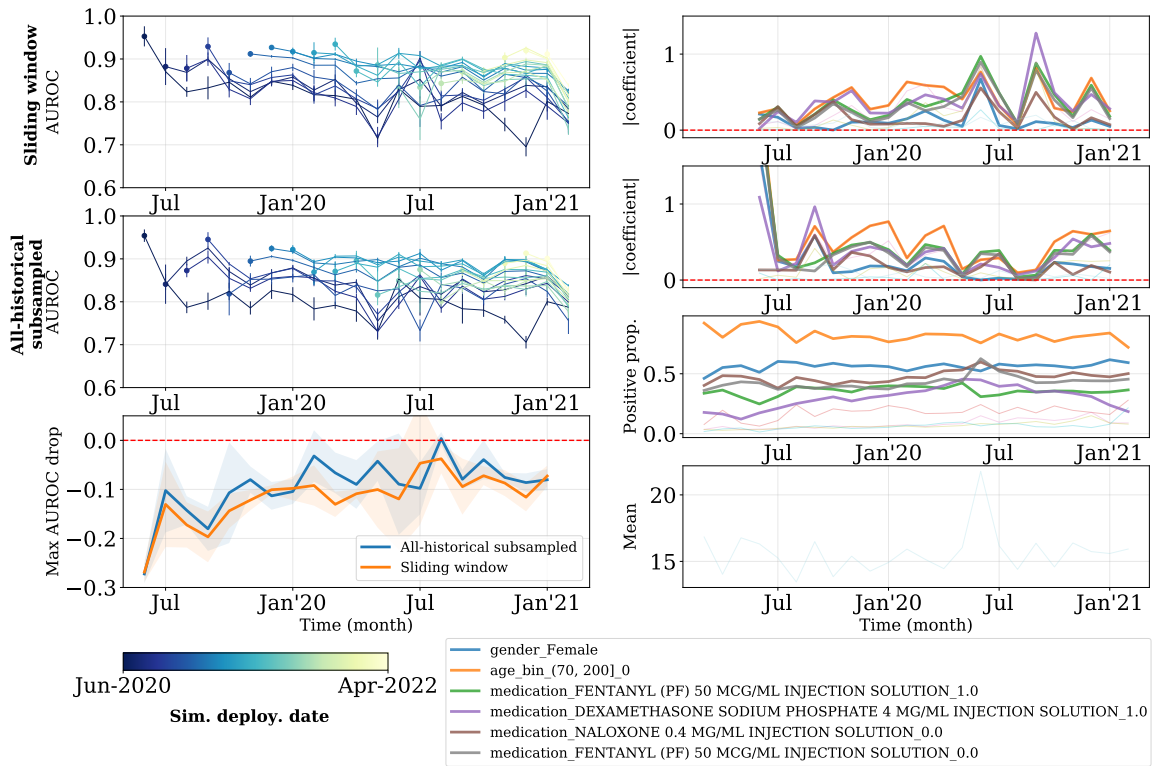


Figure 36: Diagnostic plot of SWPA COVID-19. The left column includes absolute AUROC versus time for both sliding window and all-historical subsampled, and the maximum AUROC drop for each trained model. The right column provides the absolute coefficients of each trained model from both regimes, and positive proportion of the significant features over time. One of the hypotheses for relatively large uncertainty is smaller sample size.

H.6. MIMIC-IV

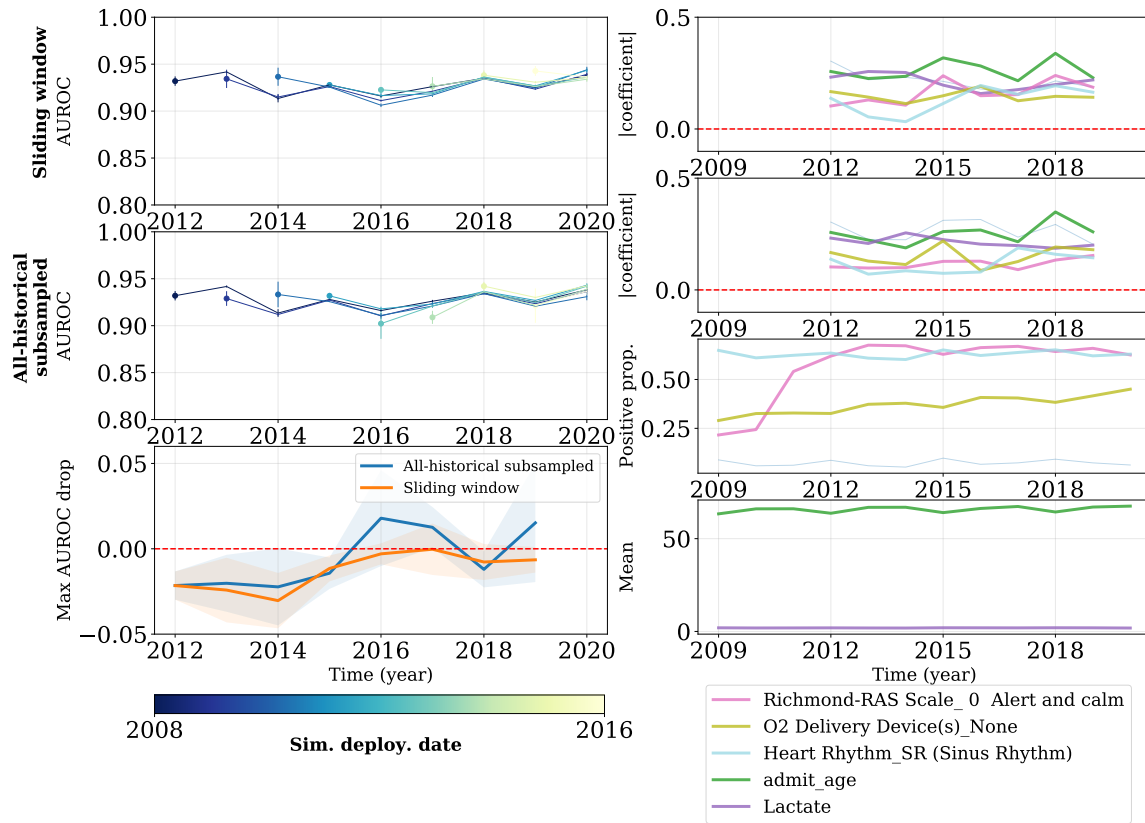


Figure 37: Diagnostic plot of MIMIC-IV. The left column includes absolute AUROC versus time for both sliding window and all-historical subsampled, and the maximum AUROC drop for each trained model. The right column provides the absolute coefficients of each trained model from both regimes, and positive proportion of the significant features over time. The model performance is relatively stable, coinciding with relatively stable distributions of a majority of important features.

H.7. OPTN (Liver)

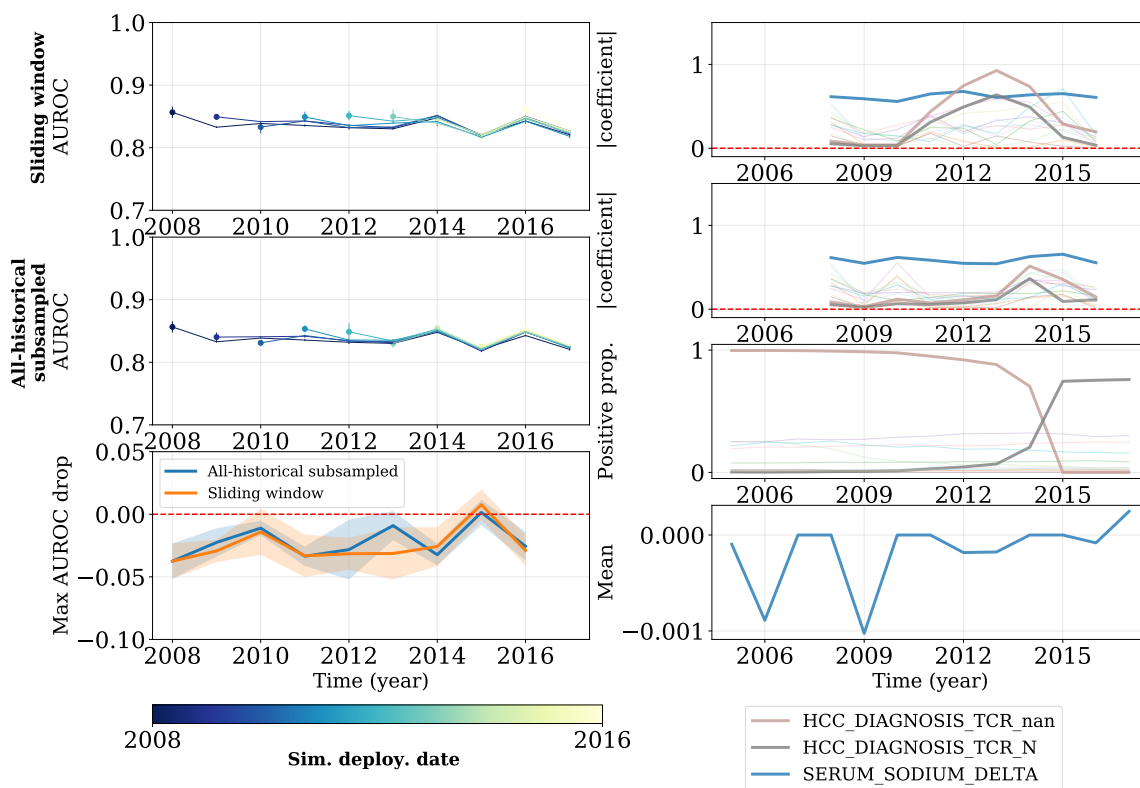


Figure 38: Diagnostic plot of OPTN (Liver). The left column includes absolute AUROC versus time for both sliding window and all-historical subsampled, and the maximum AUROC drop for each trained model. The right column provides the absolute coefficients of each trained model from both regimes, and positive proportion of the significant features over time. Although the HCC DIAGNOSIS TCR binary features change in positive proportion over time, these features were not always important, and the other important features (faded) maintain relatively stable proportions across time. Overall, model performance is quite stable over time.

Appendix I. Model performance over time (different metrics)

I.1. AUROC

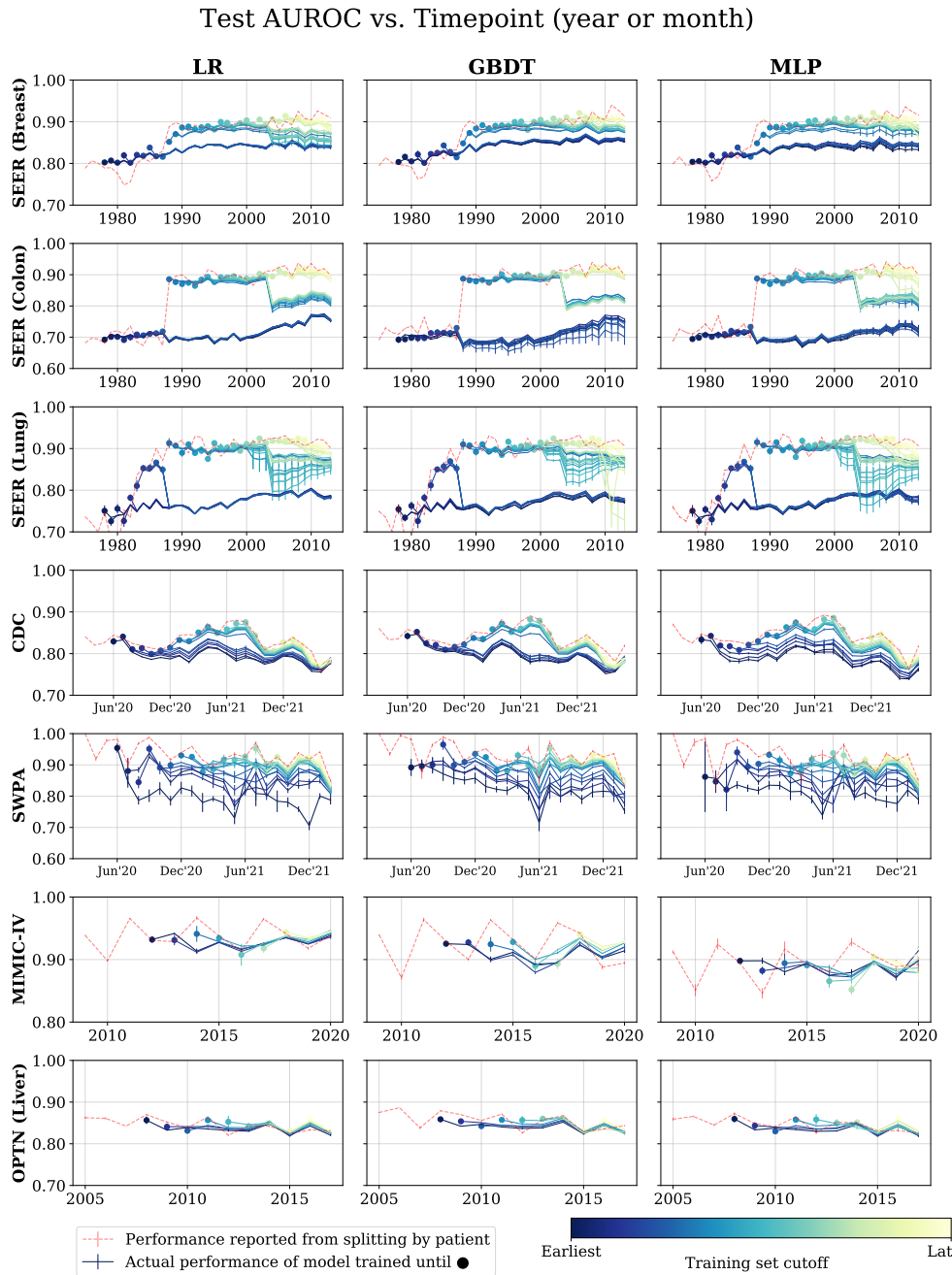


Figure 39: Absolute AUROC versus test timepoints from three model classes on all datasets.

I.2. AUPRC

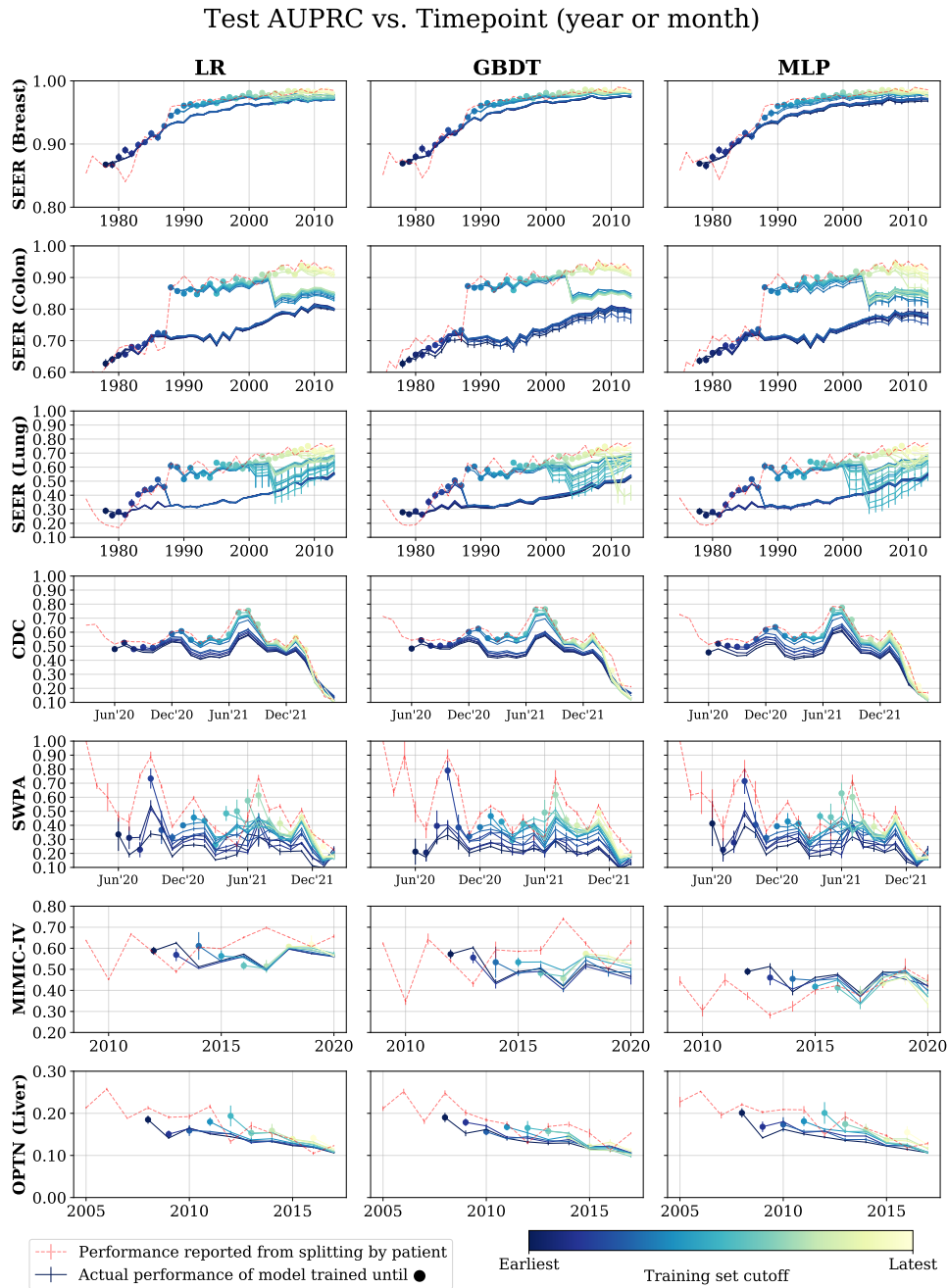


Figure 40: Absolute AUPRC versus test timepoints from three model classes on all datasets.

I.3. Accuracy

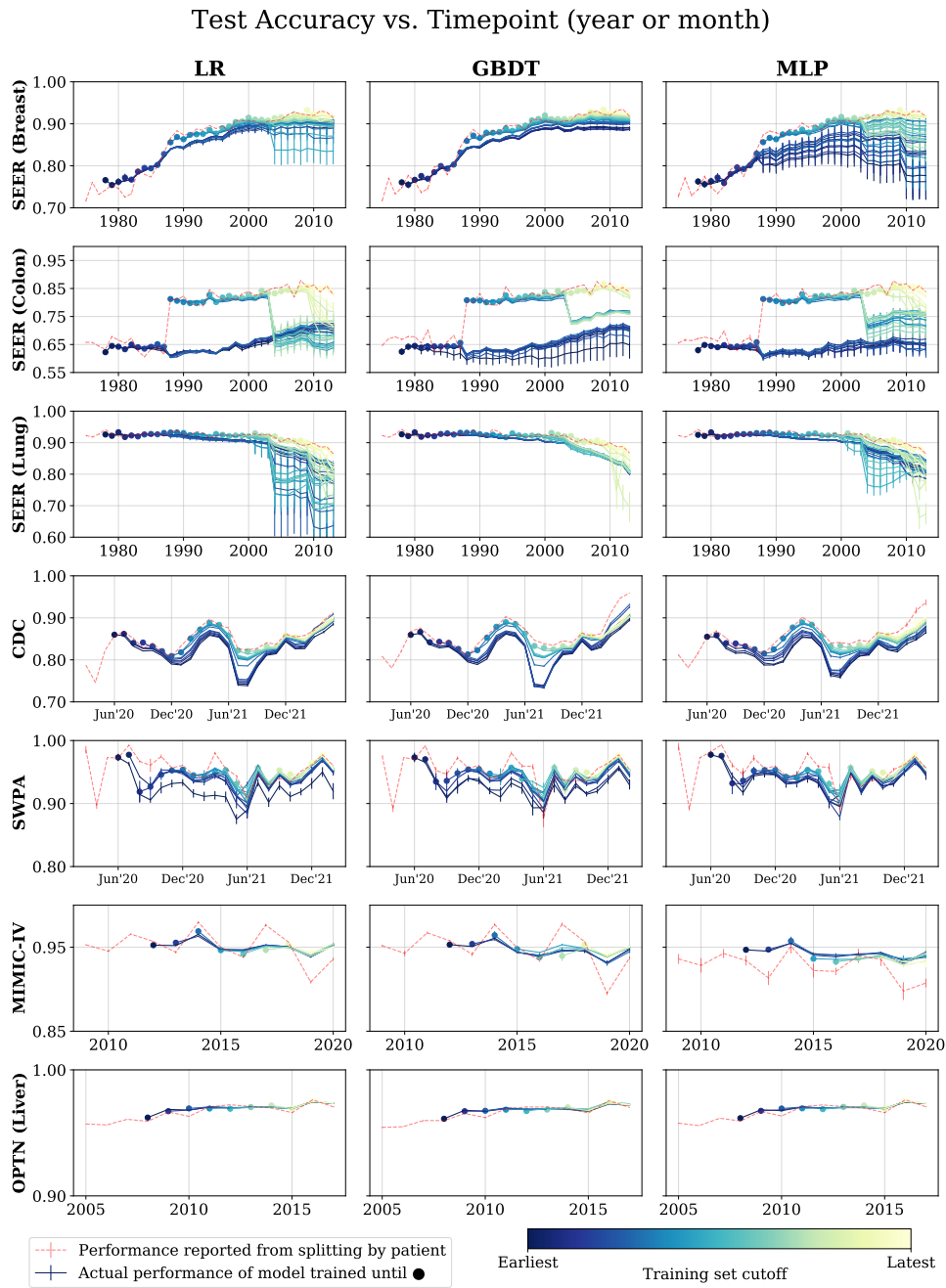


Figure 41: Absolute accuracy versus test timepoints from three model classes on all datasets.

I.4. Recall score

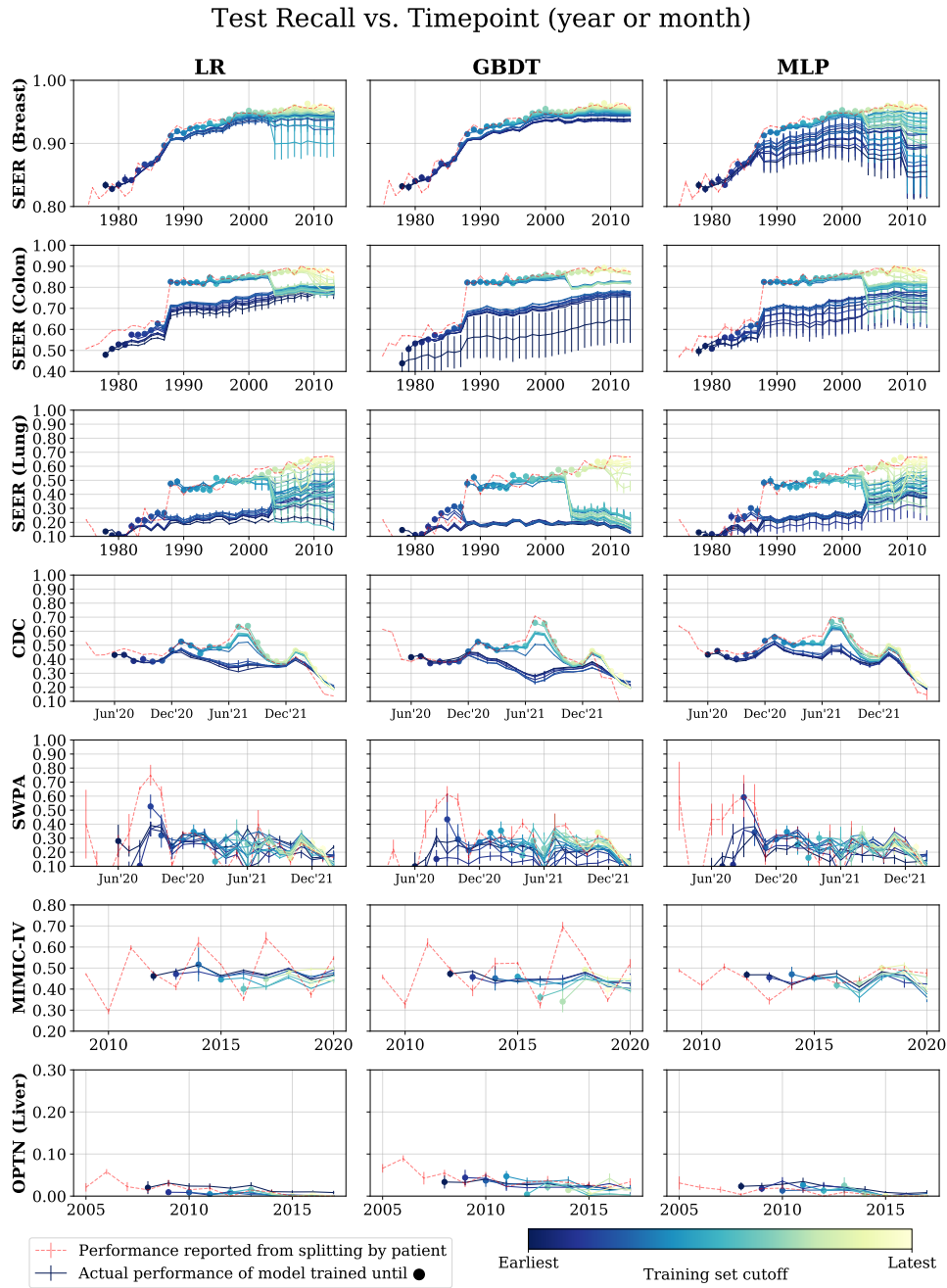


Figure 42: Absolute recall score versus test timepoints from three model classes on all datasets.

Appendix J. Hyperparameter Grids

Table 17: Hyperparameter grid for model training.

Parameter	List of searched value
LR	
C	0.01, 0.1, 1, 10, 10^2 , 10^3 , 10^4 , 10^5
GBDT	
n_estimators	50, 100
max_depth	3, 5
learning_rate	0.01, 0.1
MLP	
hidden_layer_sizes	(3,), (5,)
learning_rate_init	10^{-4} , 10^{-3} , 0.01

Appendix K. Data Split Details

Table 18: Split ratio for each dataset for training, validation and testing

Dataset	Split ratio
SEER (Breast)	0.8-0.1-0.1
SEER (Colon)	0.8-0.1-0.1
SEER (Lung)	0.8-0.1-0.1
CDC COVID-19	0.8-0.1-0.1
SWPA COVID-19	0.5-0.25-0.25
MIMIC-IV	0.5-0.25-0.25
OPTN (Liver)	0.5-0.25-0.25

Appendix L. Complete Results for All Datasets

Table 19: Test AUROC from time-agnostic evaluation (all-period training).

Model	SEER (Breast)	SEER (Colon)	SEER (Lung)	CDC	SWPA	MIMIC-IV	OPTN (Liver)
LR	0.887	0.867	0.896	0.837	0.914	0.936	0.845
GBDT	0.890	0.871	0.895	0.850	0.926	0.928	0.858
MLP	0.890	0.873	0.900	0.844	0.918	0.885	0.846

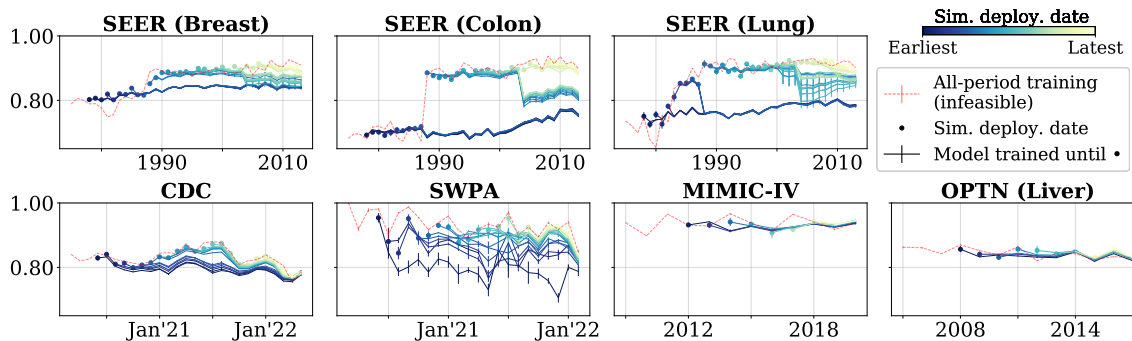


Figure 43: Average Test AUROC vs. time for LR. (GBDT and MLP plots in Appendix I.) Each solid line gives the performance of a model trained up to a simulated deployment time (marked by a dot), and evaluated across future time points. Error bars are the standard deviation of average test AUROC, computed over 5 random splits. The red dotted line gives per-time point test performance of a model from all-period training (infeasible, as it would train on data after the simulated deployment date). As the red dotted line mostly sits above the performance of any model that could have been previously deployed, standard all-period training tends to provide an over-optimistic estimate.

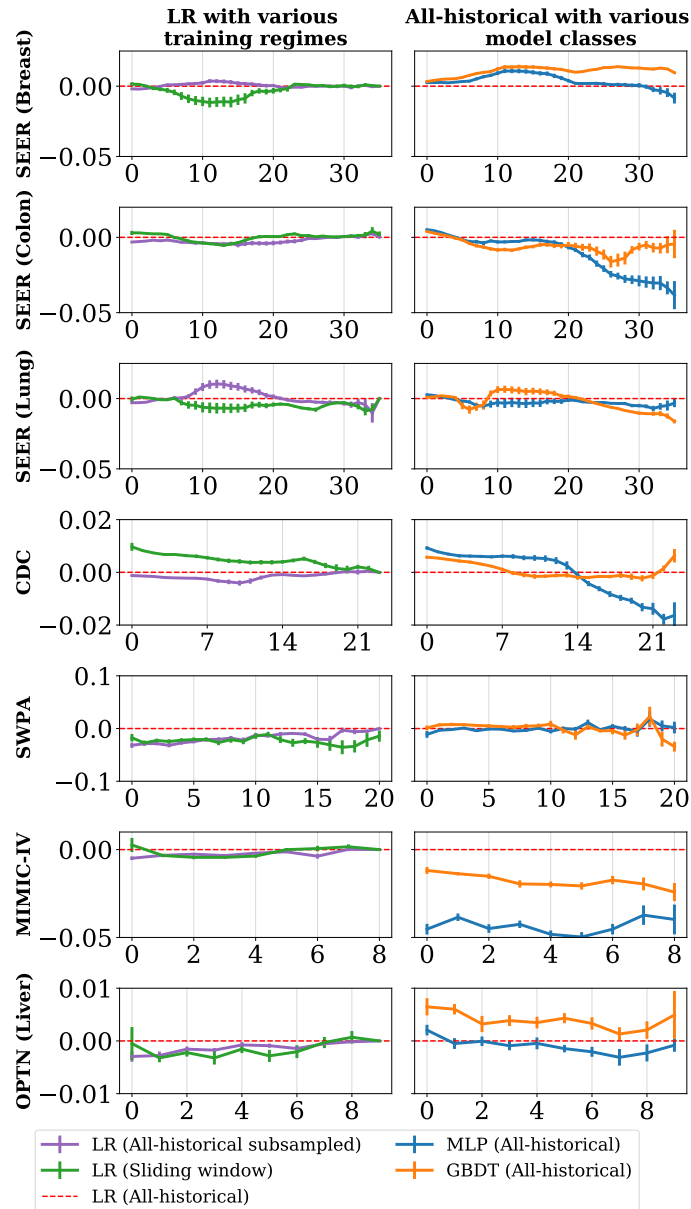


Figure 44: AUROC – AUROC_{LR All-historical} across varying stalenesses of data, for different training regimes (left) and model classes (right). Error bars are \pm std. dev.